Imaging Innovations in Cancer Research

MINI DAS

DEPARTMENT OF PHYSICS

DEPARTMENT OF BIOMEDICAL ENGINEERING

UNIVERSITY OF HOUSTON

2008 Estimated US Cancer Deaths*

Men 294,120	
Lung & bronchus	31%
Prostate	10%
Colon & rectum	8%
Pancreas	6%
Liver & intrahepatic bile duct	4%
Leukemia	4%
Esophagus	4%
Urinary bladder	3%
Non-Hodgkin lymphoma	3%
Kidney & renal pelvis	3%
All other sites	24%

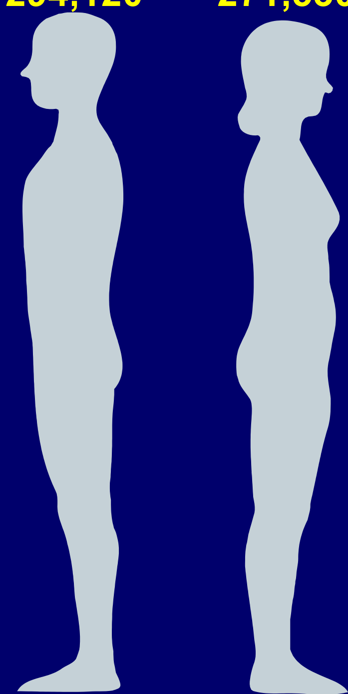

Women 271,530	
26%	Lung & bronchus
15%	Breast
9%	Colon & rectum
6%	Pancreas
6%	Ovary
3%	Non-Hodgkin lymphoma
3%	Leukemia
3%	Uterine corpus
2%	Liver & intrahepatic bile duct
2%	Brain/ONS
25%	All other sites

ONS=Other nervous system.
Source: American Cancer Society, 2008.

Cancer Death Rates* Among Women, US,1930-2004

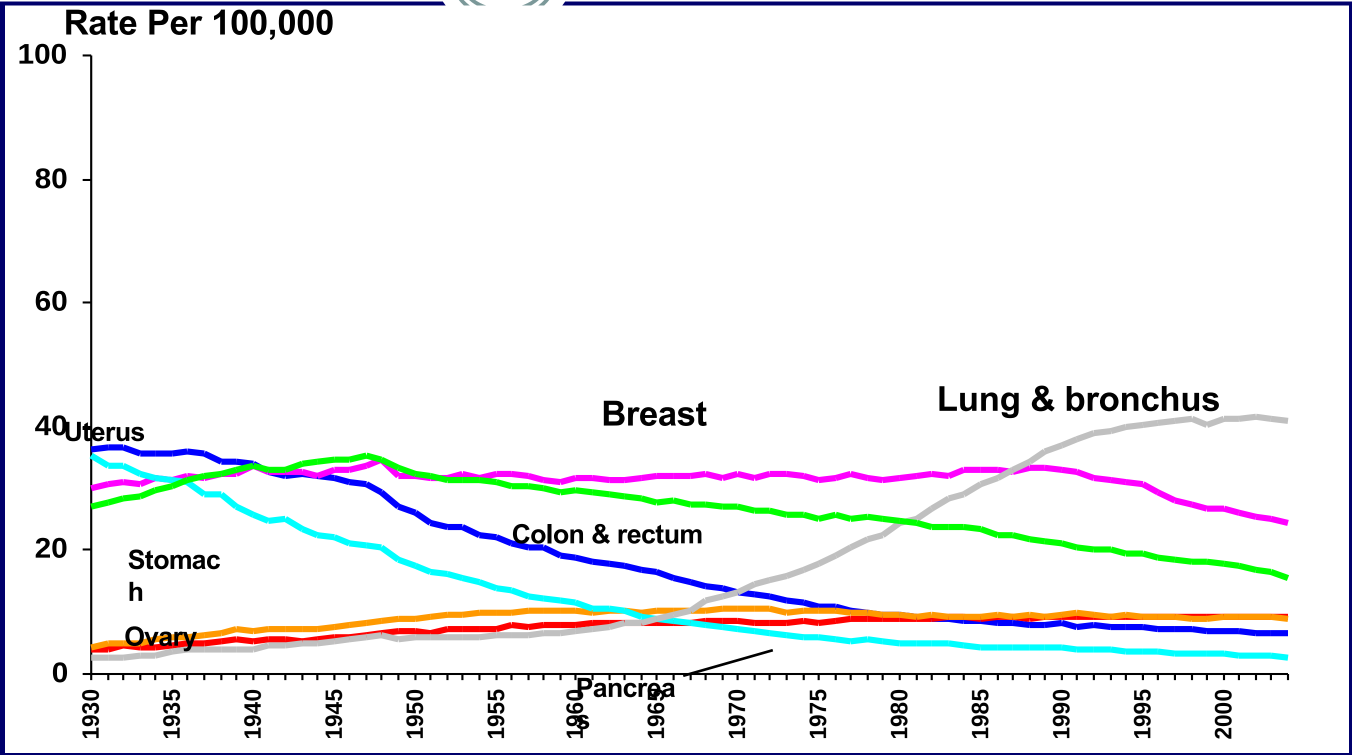

*Age-adjusted to the 2000 US standard population.
Source: US Mortality Data 1960-2004, US Mortality Volumes 1930-1959,
National Center for Health Statistics, Centers for Disease Control and Prevention, 2006.

Cancer Death Rates* Among Men, US,1930-2004

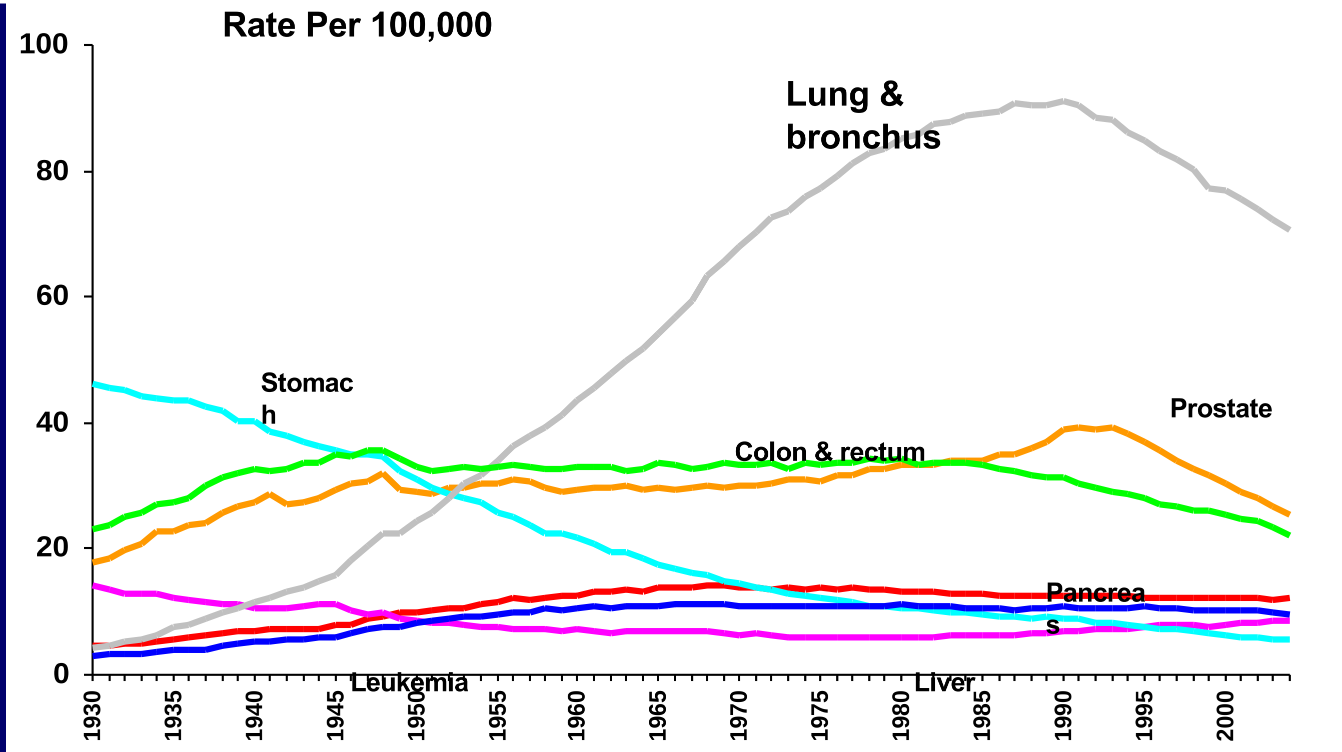

*Age-adjusted to the 2000 US standard population.
Source: US Mortality Data 1960-2004, US Mortality Volumes 1930-1959, National Center for Health Statistics, Centers for Disease Control and Prevention, 2006.

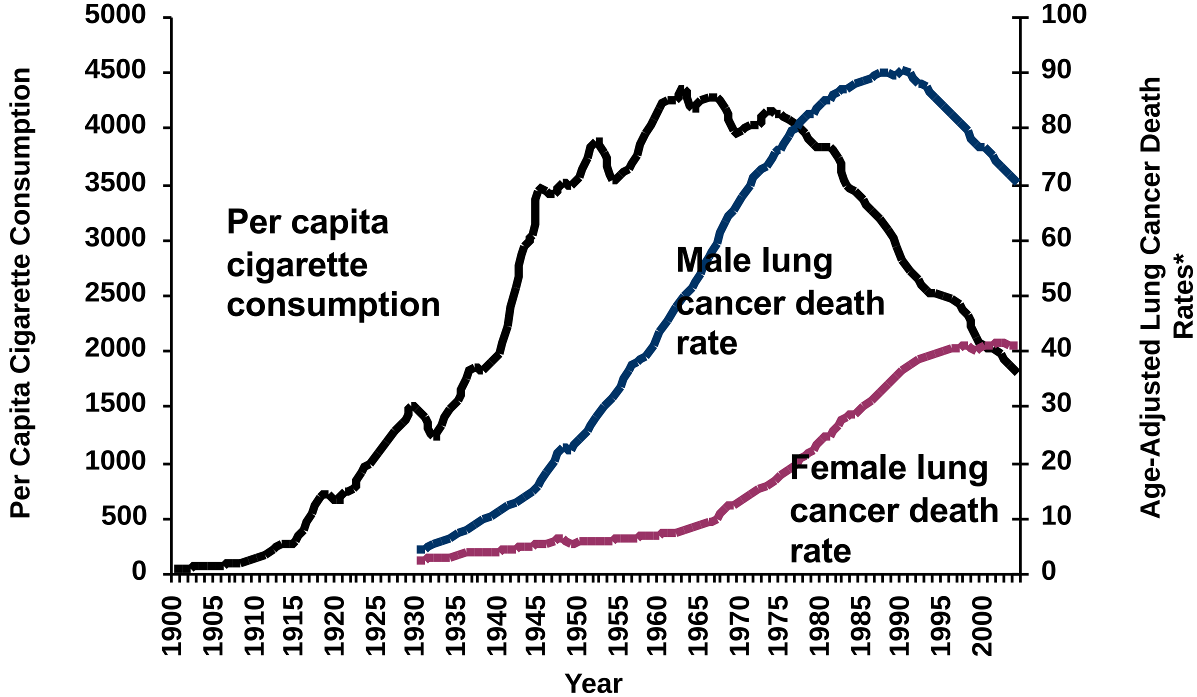

Source: Death rates: US Mortality Data, 1960-2004, US Mortality Volumes, 1930-1959, National Center for Health Statistics, Centers for Disease Control and Prevention, 2006. Cigarette consumption: US Department of Agriculture, 1900-2004.

Imaging

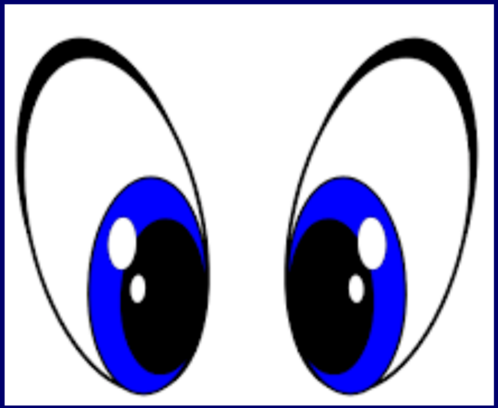

Sensing, Detection and Imaging

Photons
(optical, x-ray, γ)

Sound

Magnetic Field

Electric Field

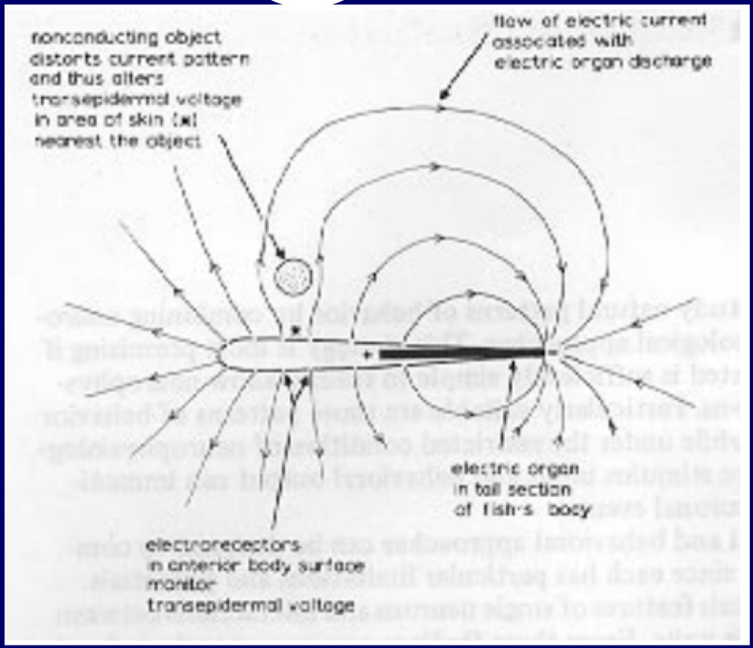

Electrolocation

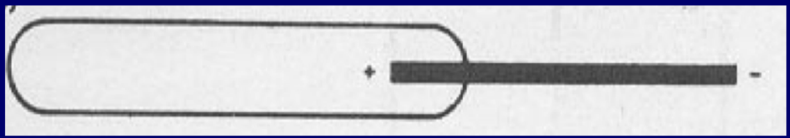

Optical Imaging

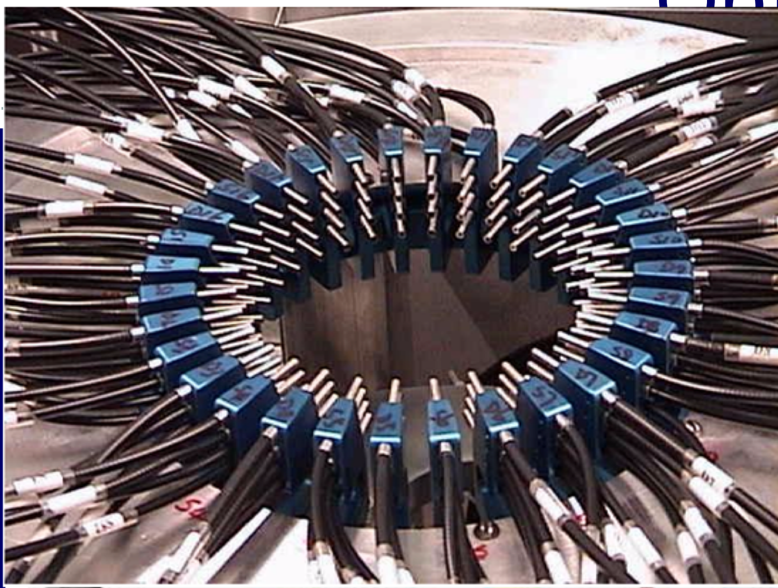

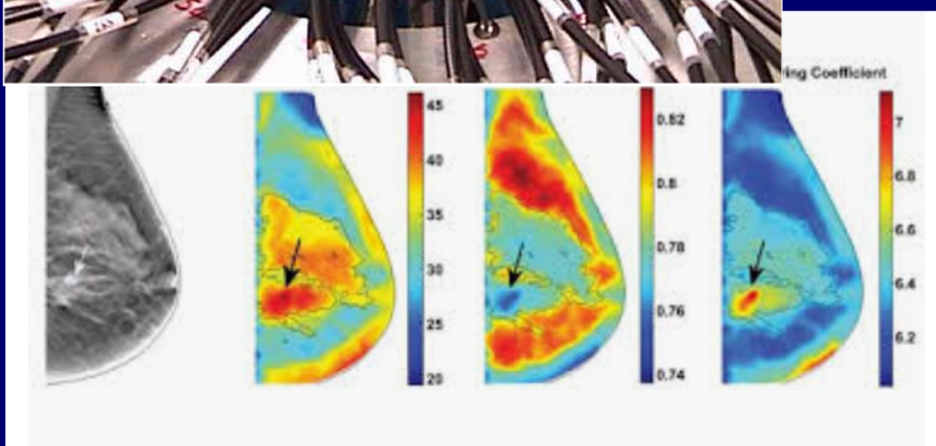

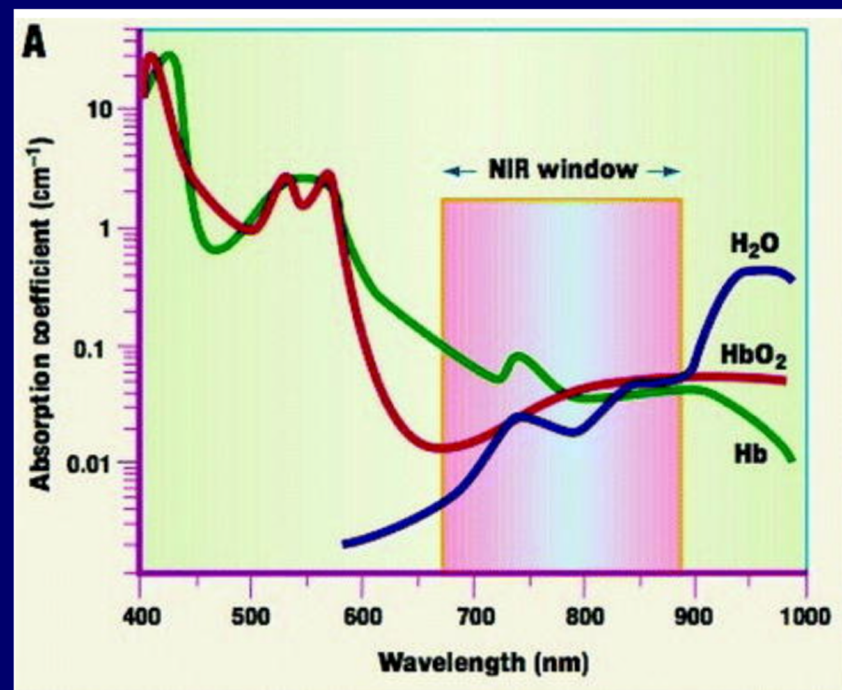

Ultrasound Imaging

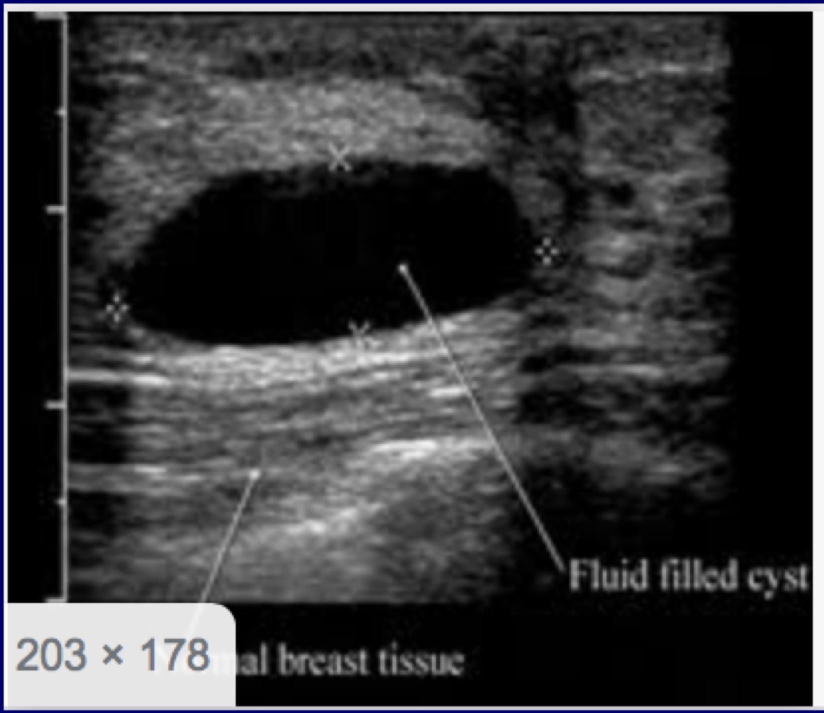

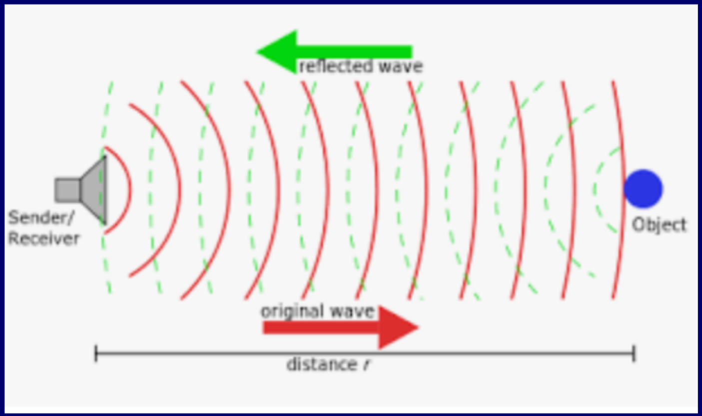

Positron Emission Tomography

Radioactive isotope

Positron emission

Gamma Rays

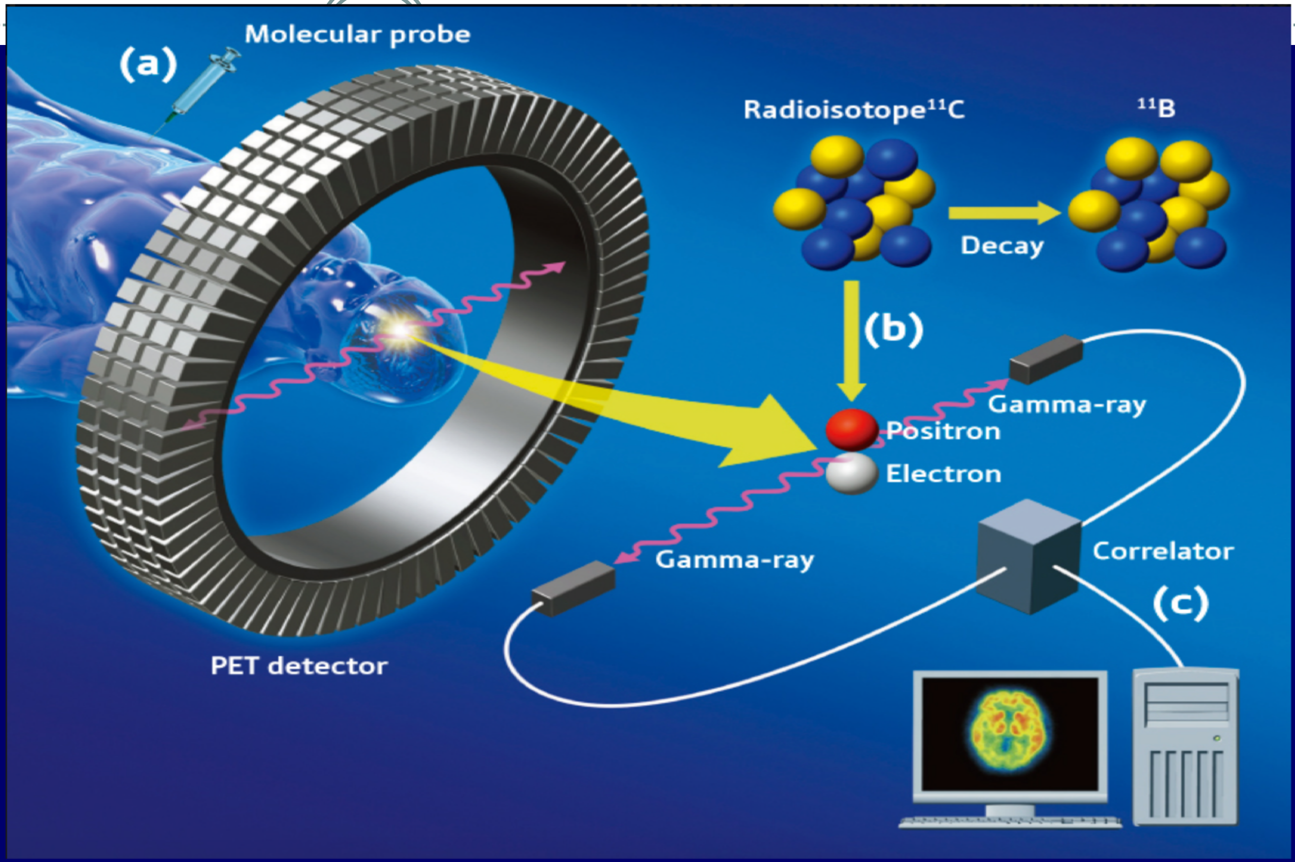

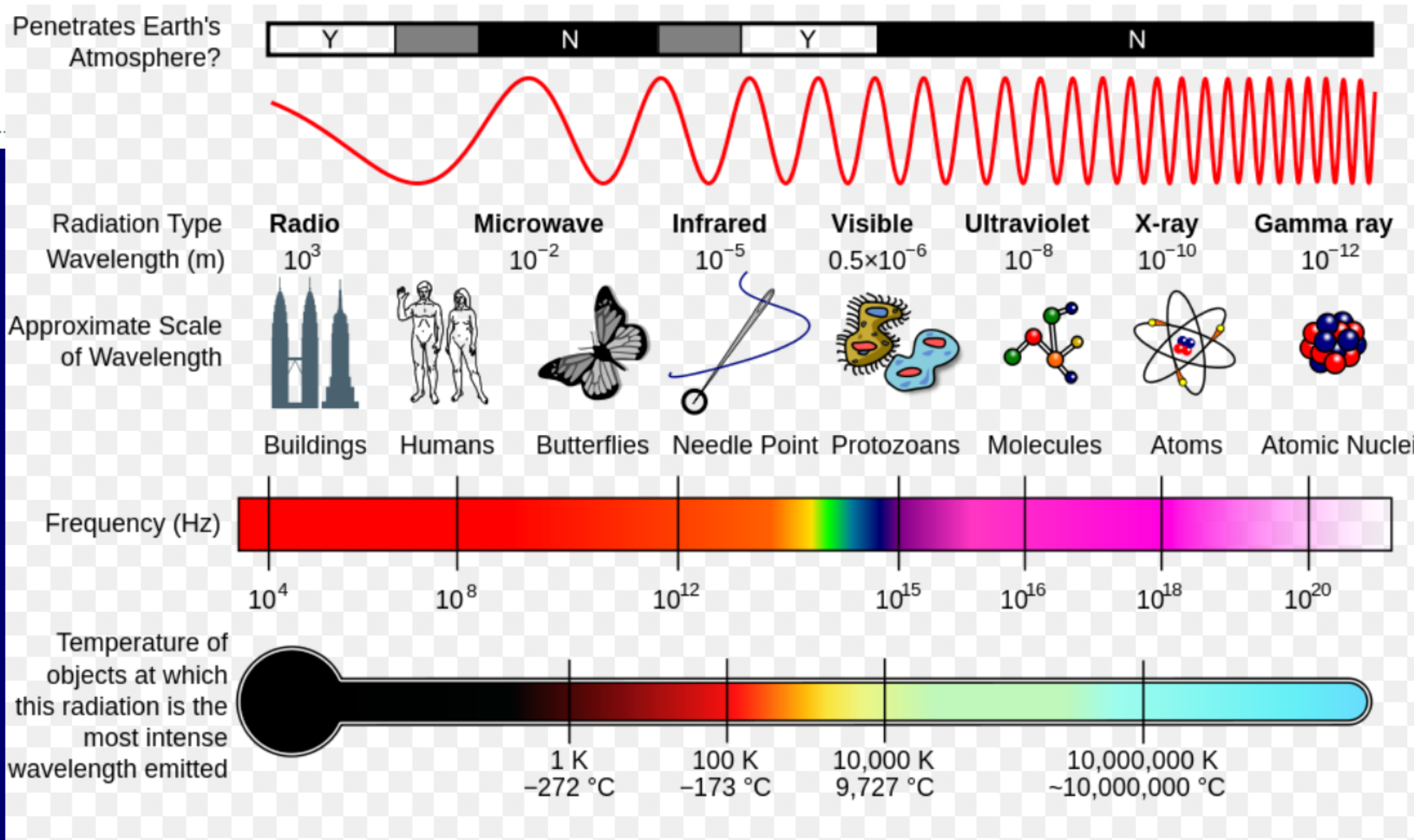
Penetrates Earth's Atmosphere?
Y
N
Y
N
Radiation Type
Wavelength (m)
Approximate Scale of Wavelength
Radio
Microwave
Infrared
Visible
Ultraviolet
X-ray
Gamma ray
10^{3}
10^{-2}
10^{-5}
0.5×10^{-6}
10^{-8}
10^{-10}
10^{-12}
Buildings
Humans
Butterflies
Needle Point
Protozoans
Molecules
Atoms
Atomic Nuclei
Frequency (Hz)
10^{4}
10^{8}
10^{12}
10^{15}
10^{16}
10^{18}
10^{20}
Temperature of objects at which this radiation is the most intense wavelength emitted
1 K
−272 °C
100 K
−173 °C
10,000 K
9,727 °C
10,000,000 K
~10,000,000 °C

Once upon a time...

Photoelectric Effect

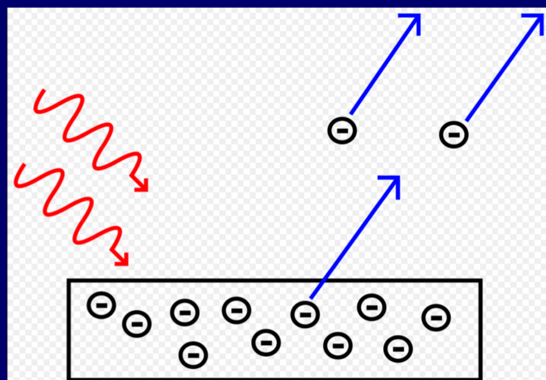

Photoelectric effect (1905)

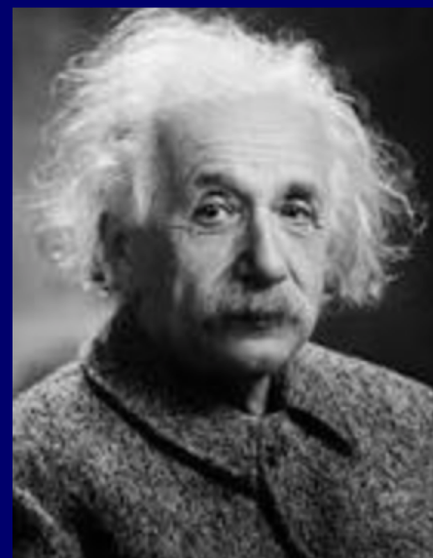

1921-Physics- ..discovery of laws of PE

Compton Scattering (Inelastic)

Nobel Prize
in Physics (1927)

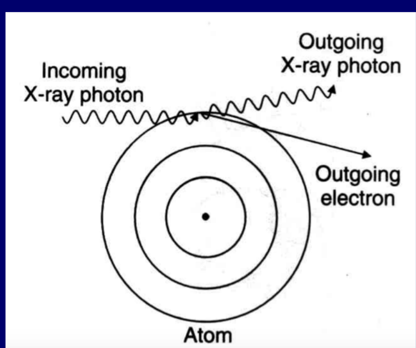

A QUANTUM THEORY OF THE SCATTERING OF X-RAYS BY LIGHT ELEMENTS

By Arthur H. Compton

Abstract

A quantum theory of the scattering of X-rays and γ-rays by light elements. —The hypothesis is suggested that when an X-ray quantum is scattered it spends all of its energy and momentum upon some particular electron. This electron in turn scatters the ray in some definite direction. The change in momentum of the X-ray quantum due to the change in its direction of propagation results in a recoil of the scattering electron. The energy in the scattered quantum is thus less than the energy in the primary quantum by the kinetic energy of recoil of the scattering electron. The corresponding *increase in the wave-length of the scattered beam* is $\lambda_\theta - \lambda_0 = (2h/mc) \sin^2 \frac{1}{2}\theta = 0.0484 \sin^2 \frac{1}{2}\theta$, where h is the Planck constant, m is the mass of the scattering electron, c is the velocity of light, and θ is the angle between the incident and the scattered

Arthur H. Compton, The Physical Review (May 1923)

Attenuation

$$I_m(x,y,E_n) = I_0(x,y,\ E_n)\exp(-\int \mu(\mathbf{r},E_n)\,dz)$$

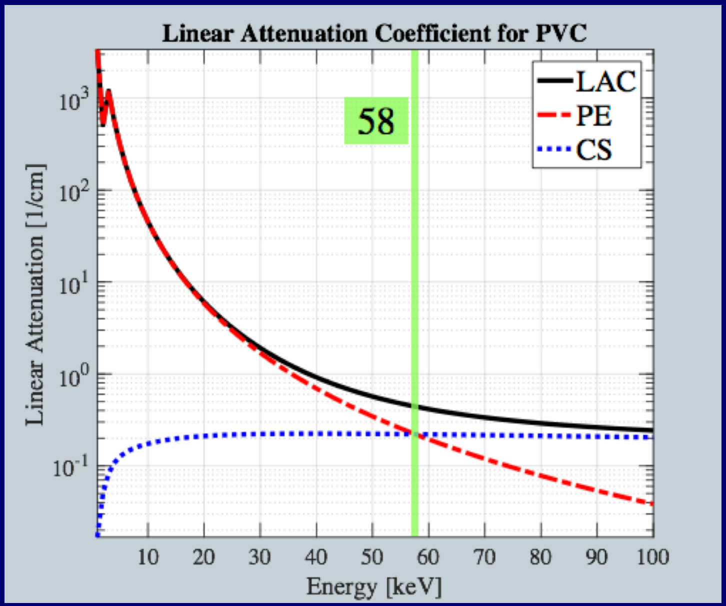

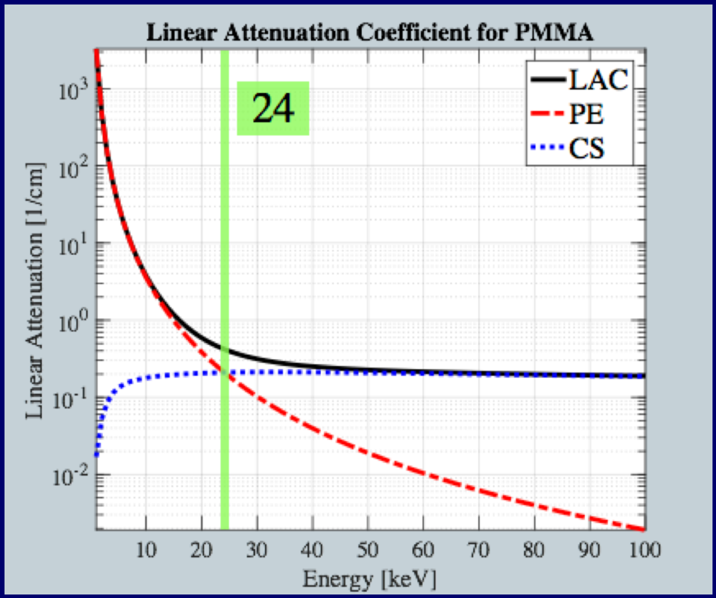

National Institute for Standards and Technology (NIST)

Mammography- Low Tissue Contrast

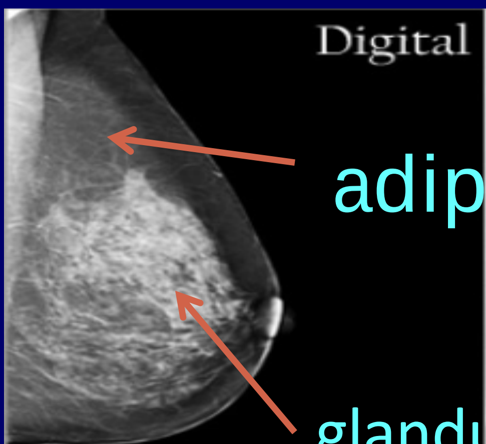

adipose

glandular

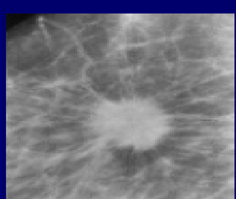

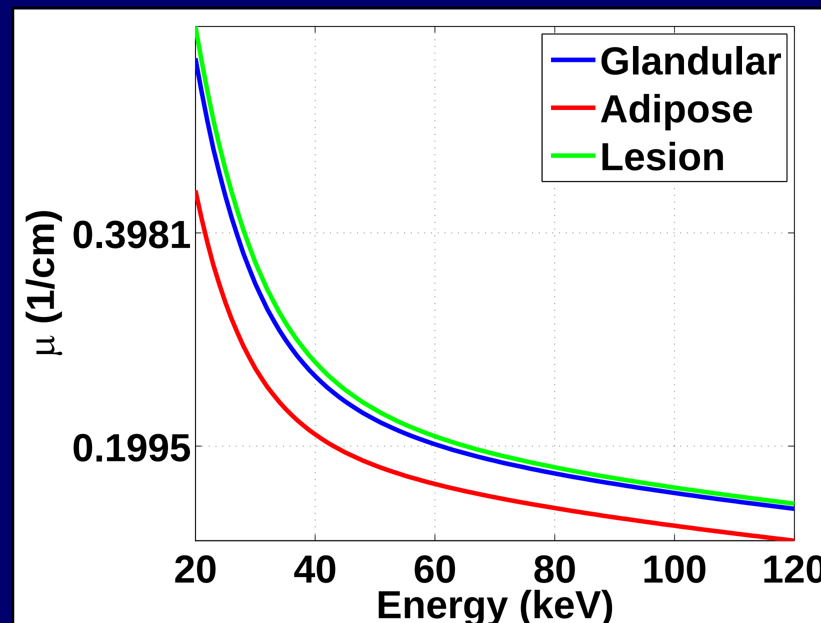

Spiculated Mass

Microcalcification cluster

Example of Missed Lesion

Invasive Ductal Carcinoma

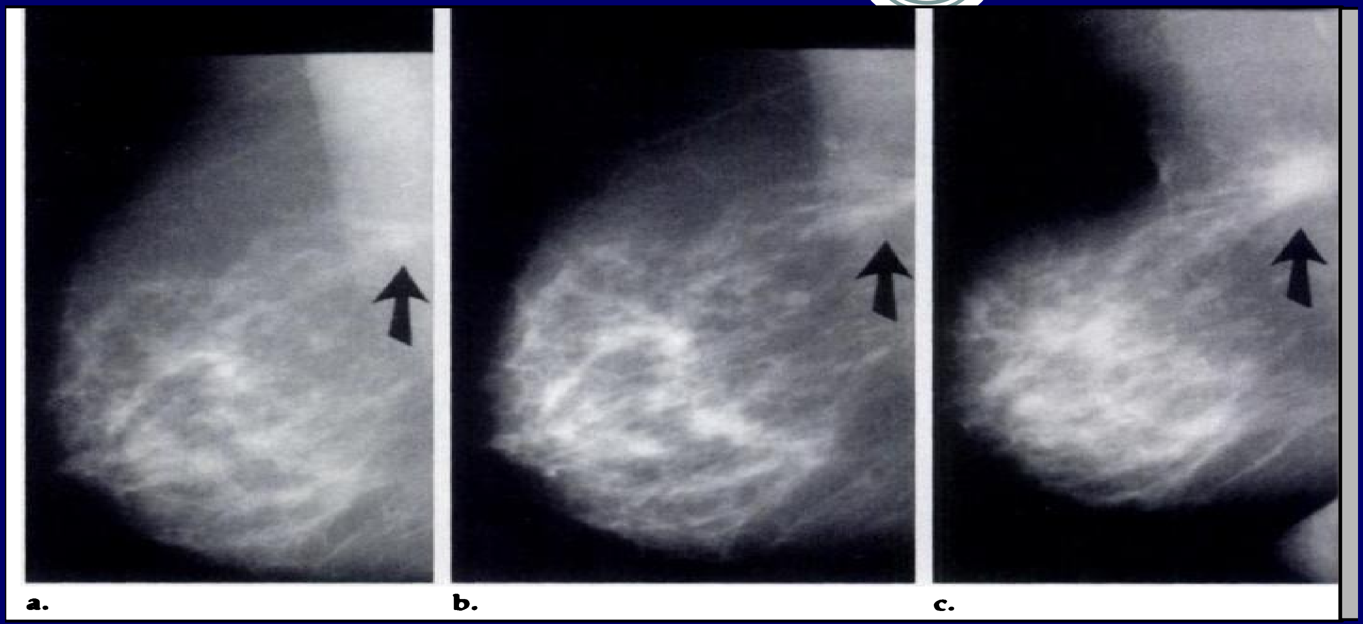

Years: 1985 1987 1988

Adapted from Bird et al. ,*Radiology, 184 (3)* (1992)

Digital Breast Tomosynthesis

Potential to Reduce False-Negative Diagnosis

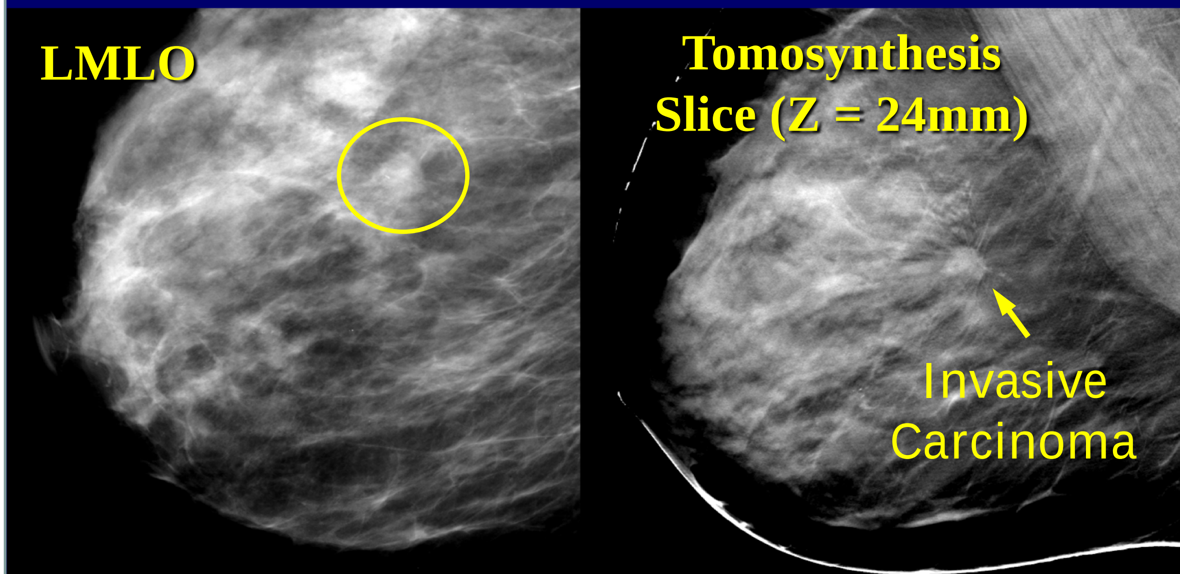

D. B. Kopans, MGH

Computed Tomography (CT)

Radon Transform

Inverse Radon

Image Reconstruction

Filtered Back Projection

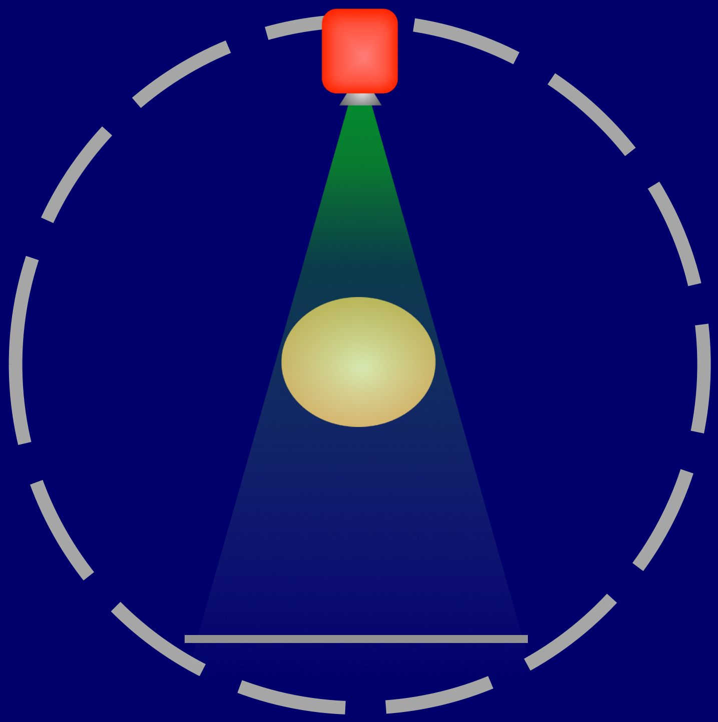

Zernike

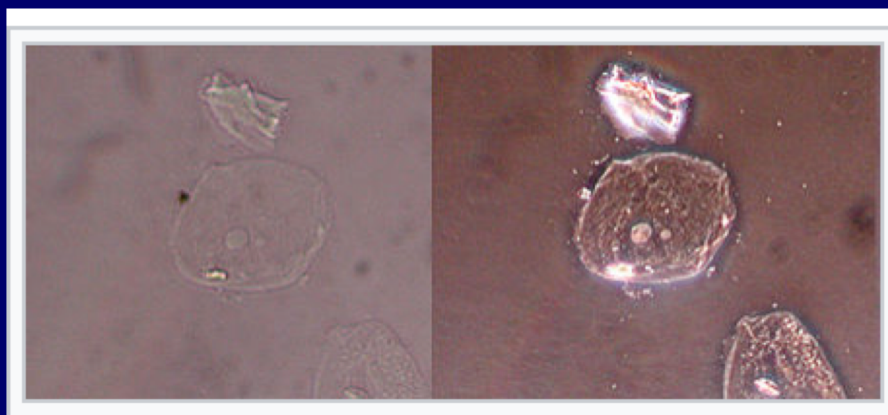

Frits Zernike
Physics Nobel Prize 1953
Phase contrast optical microscope

Wave Nature of X-Rays

Max Von Laue
Physics- 1914

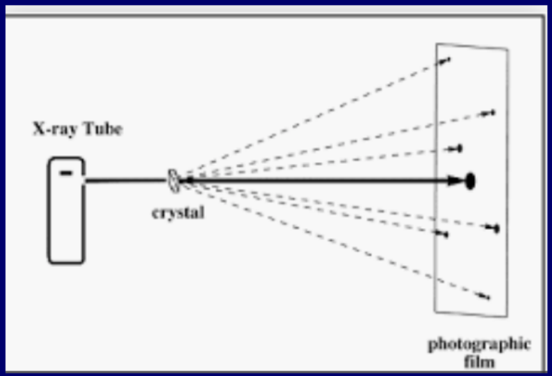

Interference

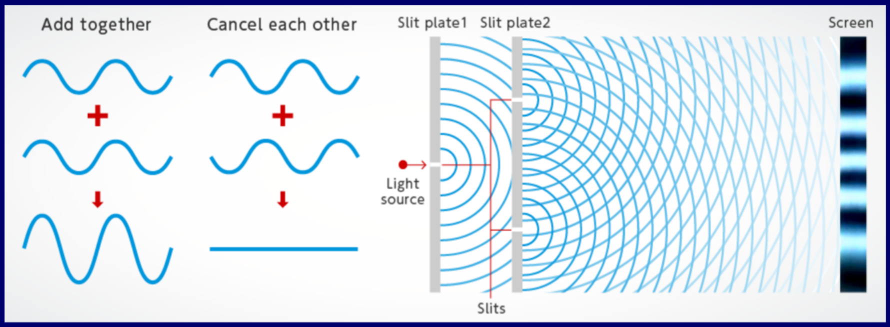

X-Ray Phase-Contrast Imaging (PCI)

Phase changes (or refractive properties) – contrast mechanism

$$n(E) = 1 - \delta(E) - i\beta(E)$$

Phase Absorption

$$\delta(E) >> \beta(E)$$

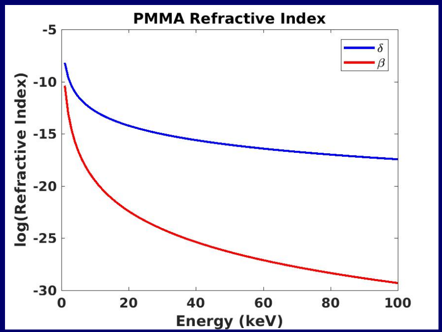

$$\mu = -\frac{4\pi}{\lambda}\int \beta(z)dz$$

Effective atomic number

$$\phi = -\frac{2\pi}{\lambda}\int \delta(z)dz$$

Electron density

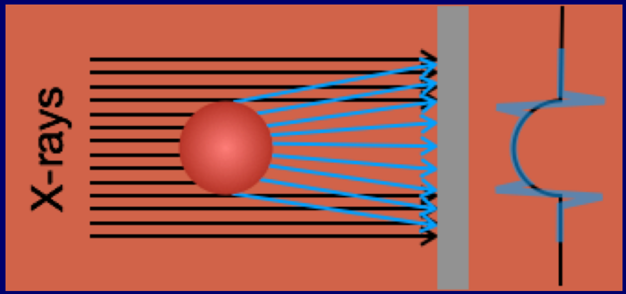

Potential to image at high energy (low dose)

In-Line Propagation PCI

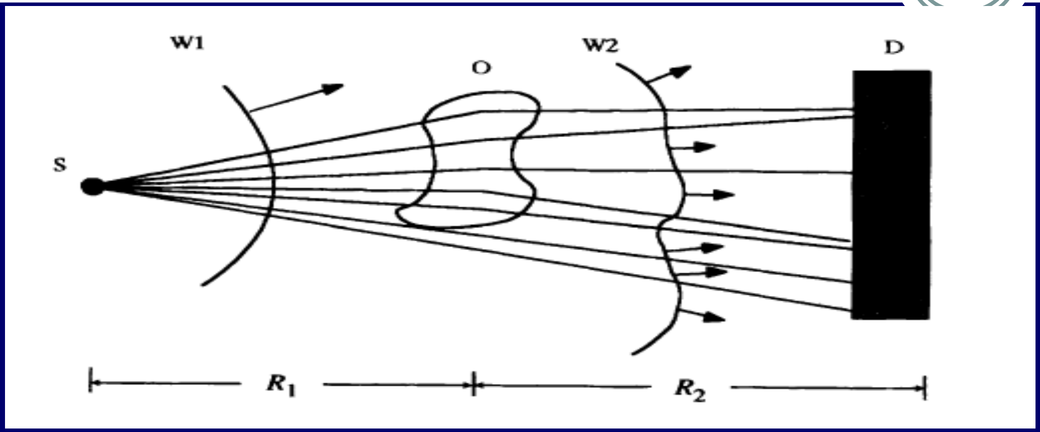

Wilkins, Nature (1996)

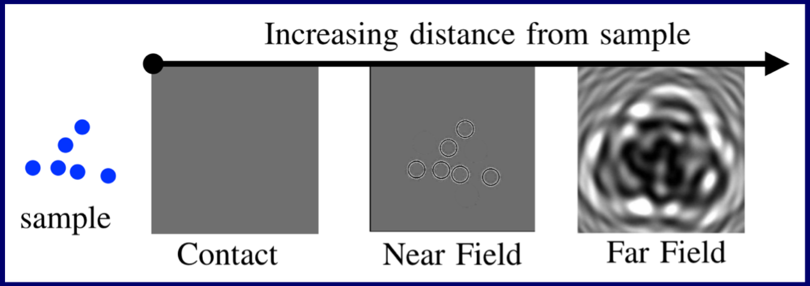

Wave-front distortions due to the object leads to intensity modulations

Requires: High coherence x-ray source,
High resolution detectors (tens of μm)

Grating Interferometry PCI

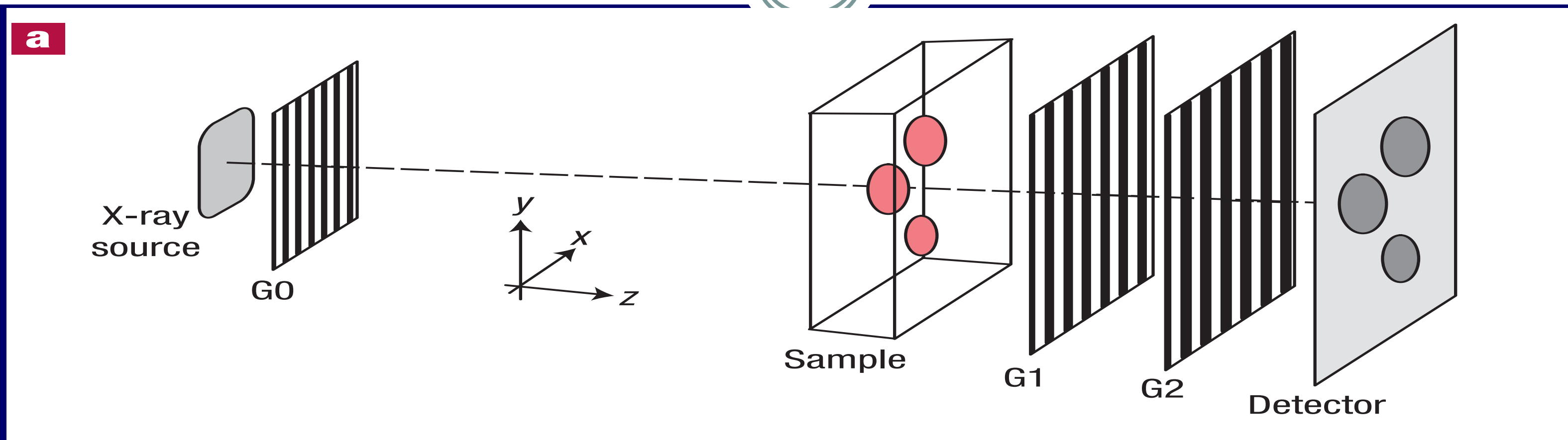

Talbot-Lau interferometer
Multiple highly precise measurements required
Requires gratings of very small period < 5μm

Pfeiffer et al, Nature (2006)

Coded-Aperture (CA) PCI

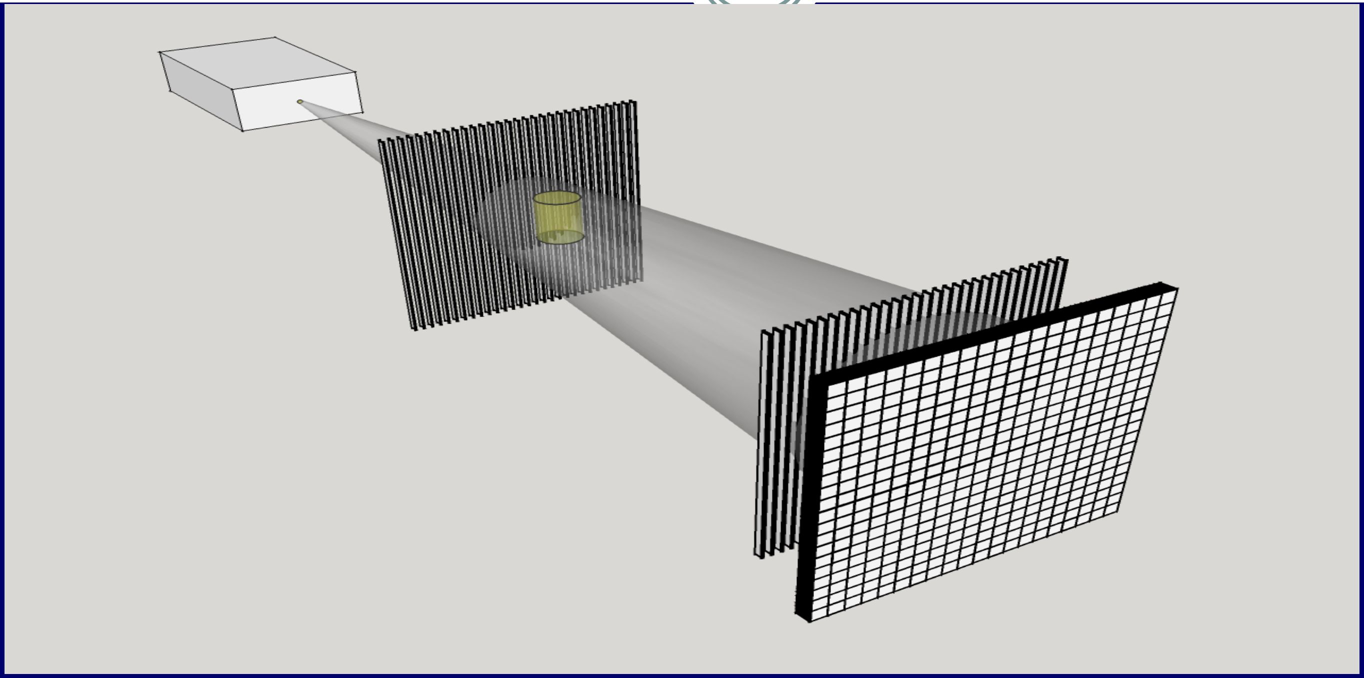

A. Olivo, UC London

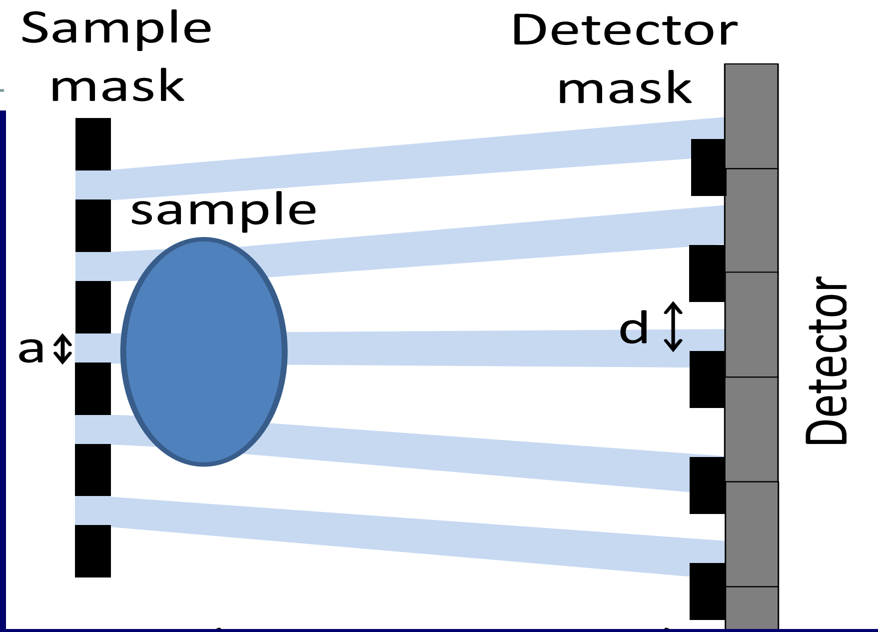

An edge-illumination effect is created using a pair of mutually displaced masks
- Refraction effect ; not Interference

PCI Image

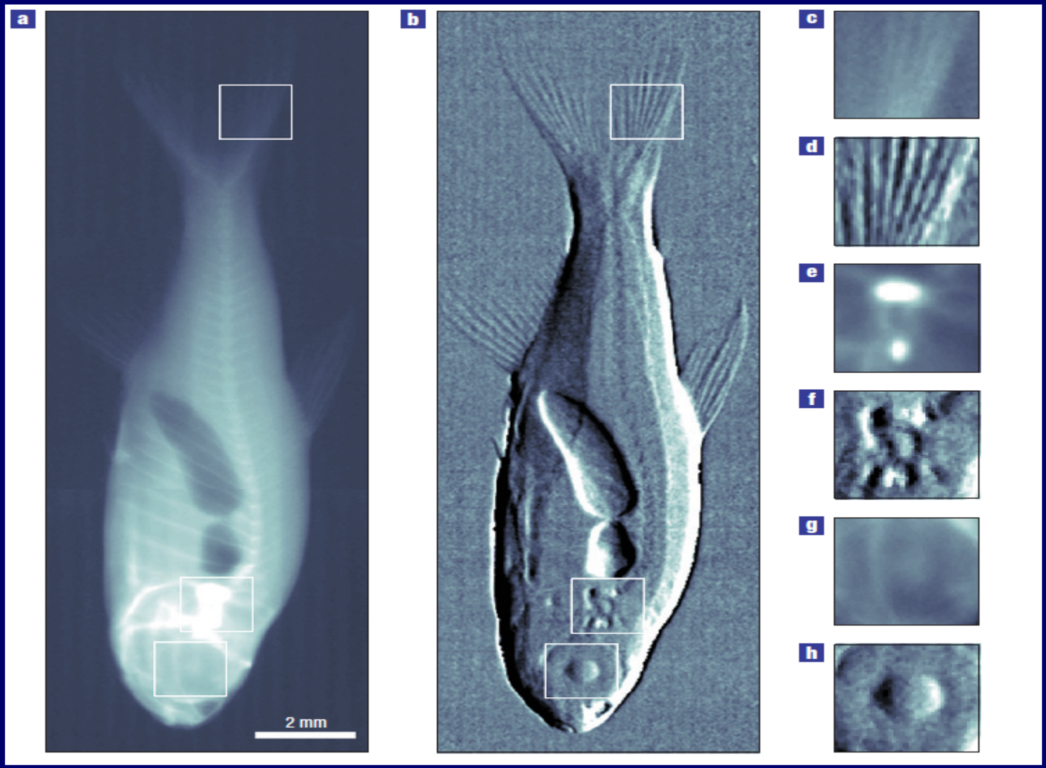

Pfeiffer et al, Nature (2006)

Effect of Object Thickness on PCI Signal

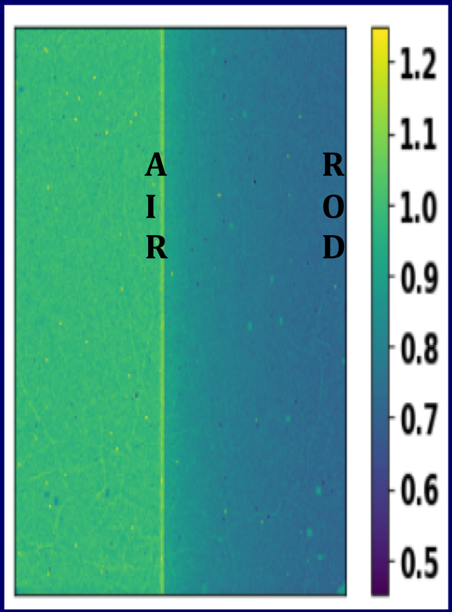

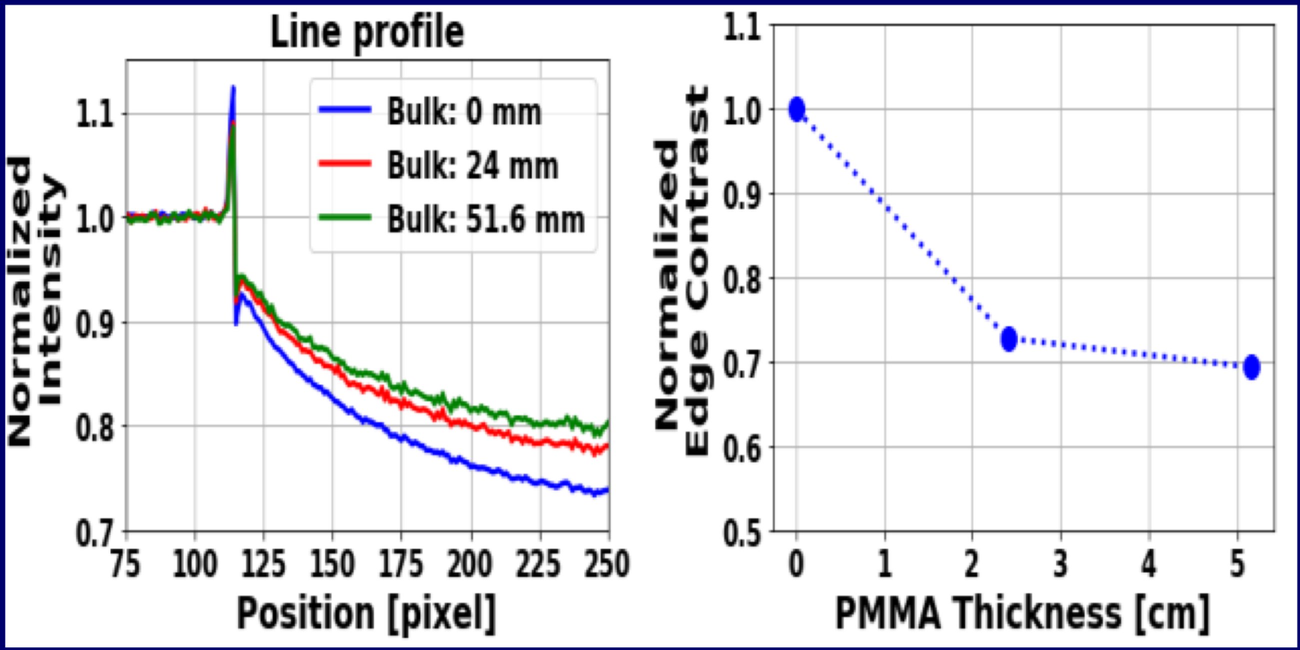

Zebra Fish- Spectral PCI

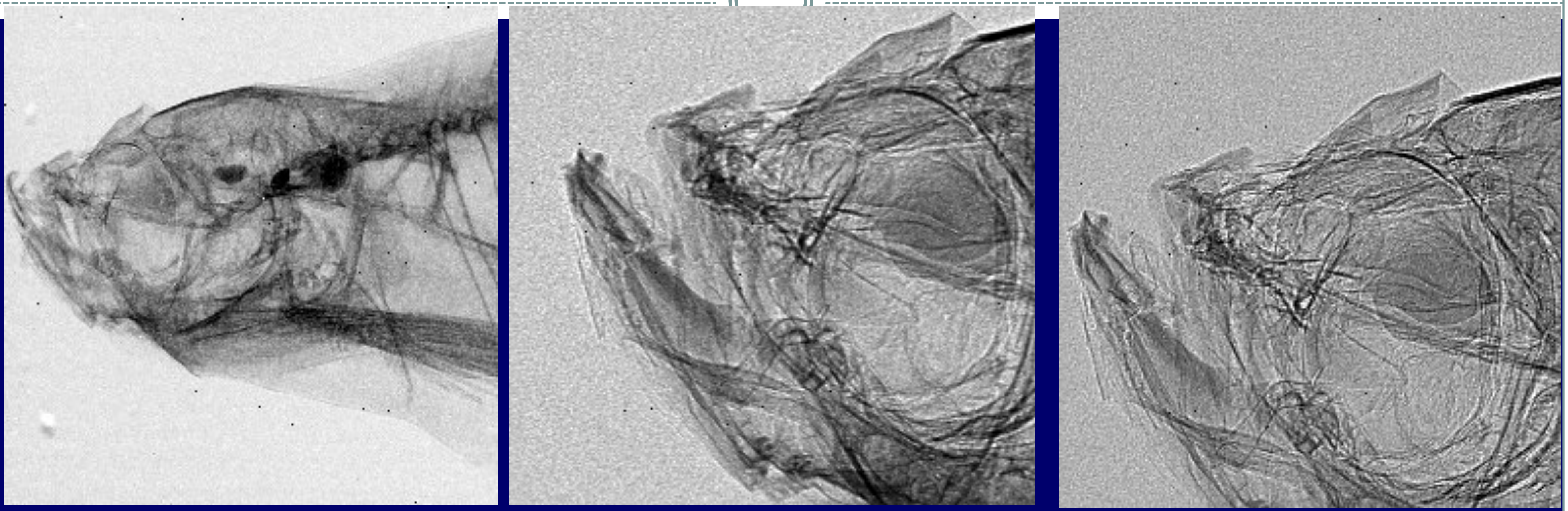

Non-Phase Contrast

Phase Contrast ~25keV

Phase Contrast 30-100keV

Spectral Phase Retrieval

- Absorption and phase change due to propagation creates intensity variations

$$\frac{2\pi}{\lambda}\frac{\partial I}{\partial z} = -\nabla.(I\nabla\phi)$$

$$\mathrm{I}(R_2, E) = I(R_1, E)\left(1 - \frac{R_2\nabla^2\phi}{k}\right)$$

$$\mathrm{I}(R_1, E) = I_0(R_1, E)\exp\left(-\int \mu(E)dz\right)$$

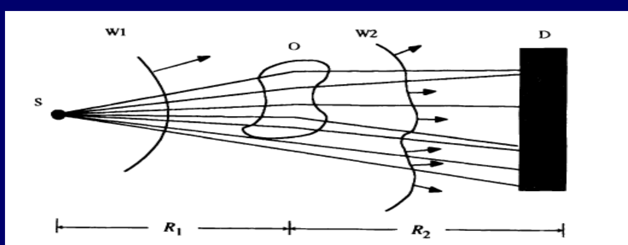

Gursoy, Das (2013)

$$\mu(E) = NK\frac{Z^5}{e^3(E)} + NZ\sigma_{\mathrm{KN}}(E)$$

Photoelectric

Compton Scatter

Single-Step Spectral PCI

Gursoy and Das, Optics Letters (2013)

Estimated

Ground Truth

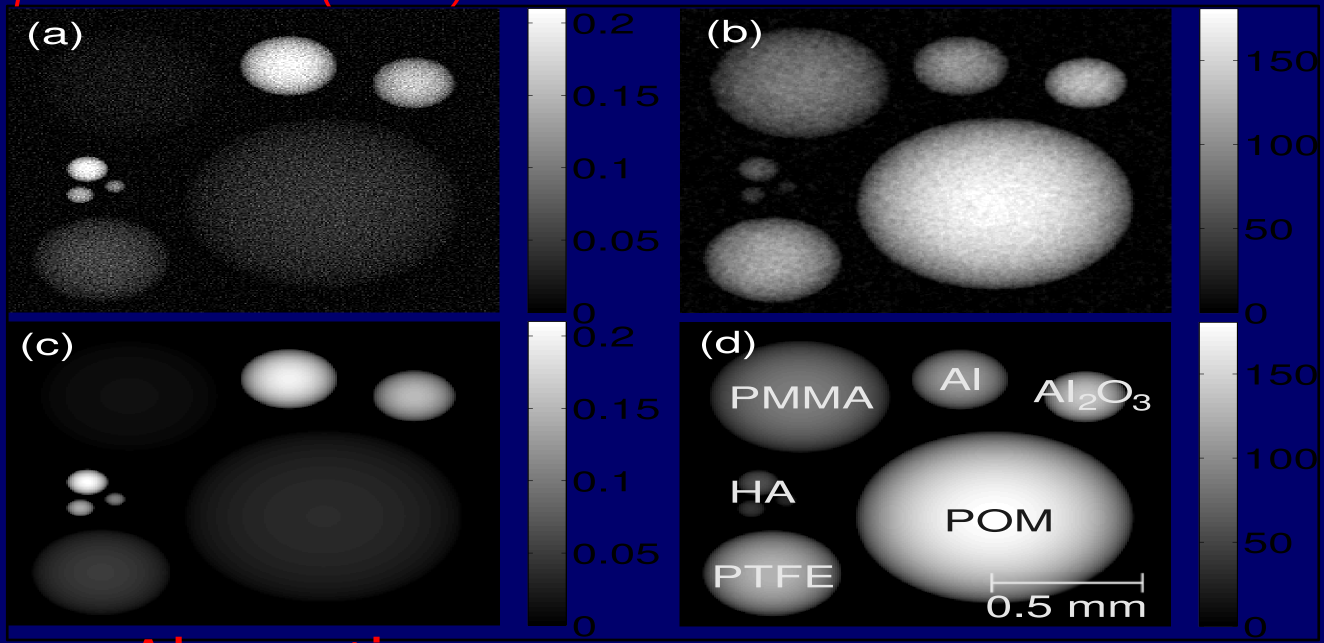

Absorption

Phase

~ Effective Atomic Number

~ Electron Density

May 1, 2013 / Vol. 38, No. 9 / OPTICS LETTERS 1461

Single-step absorption and phase retrieval with polychromatic x rays using a spectral detector

Doğa Gürsoy and Mini Das*

Department of Physics, University of Houston, Houston 77204, USA

**Corresponding author: mdas@uh.edu*

Received January 17, 2013; revised March 17, 2013; accepted March 19, 2013;
posted April 2, 2013 (Doc. ID 183047); published April 26, 2013

In this Letter, we present a single-step method to simultaneously retrieve x-ray absorption and phase images valid [redacted]

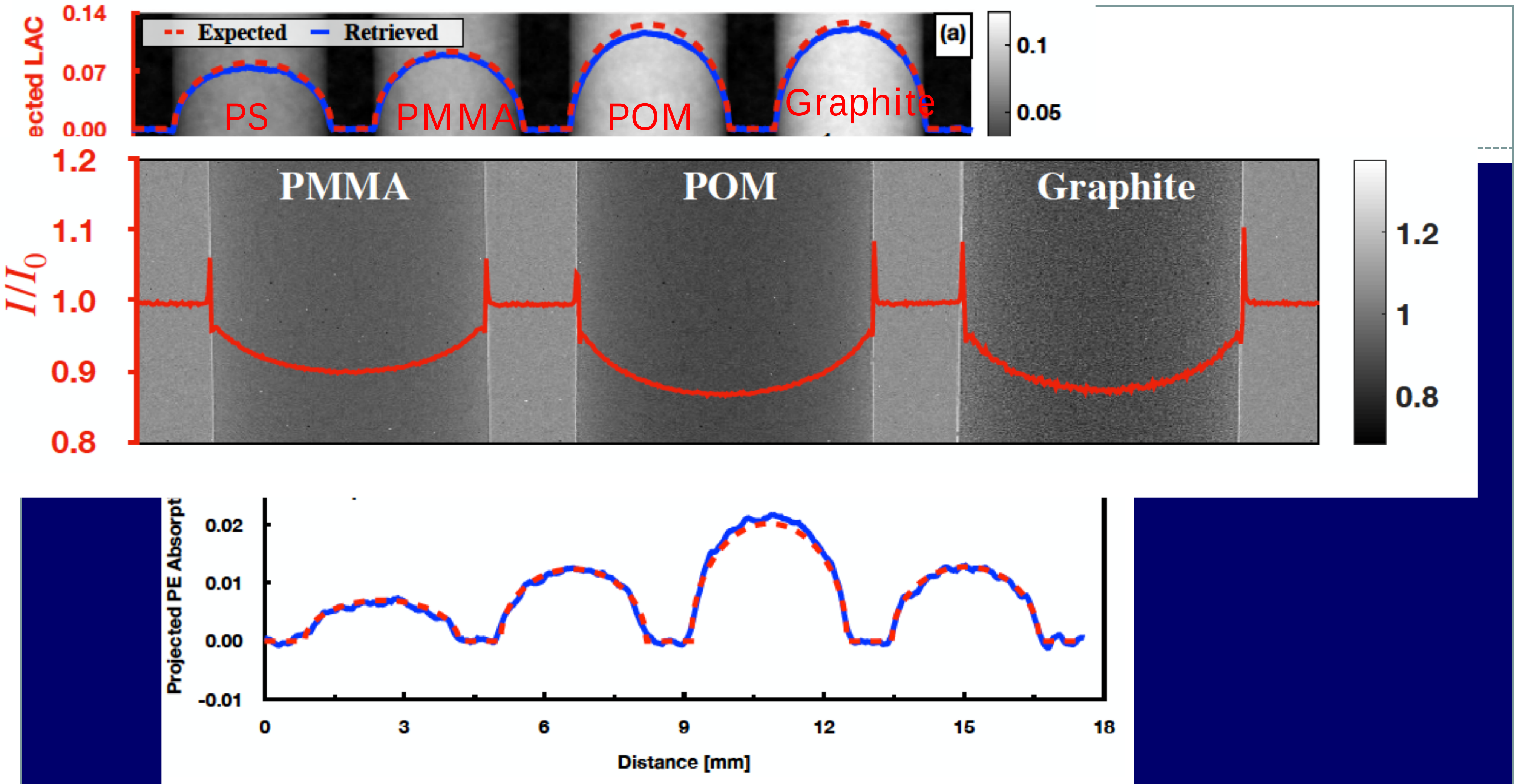

ected LAC
0.14
0.07
0.00
Expected
Retrieved
(a)
PS
PMMA
POM
Graphite
0.1
0.05
I/I_0
1.2
1.1
1.0
0.9
0.8
PMMA
POM
Graphite
1.2
1
0.8
Projected PE Absorpt
0.02
0.01
0.00
-0.01
0
3
6
9
12
15
18
Distance [mm]

Single-Step Retrieval of Absorption, Phase and Differential Phase *(Projection Image)*

True

Signals in 5cm thick breast-like soft tissue

Retrieved

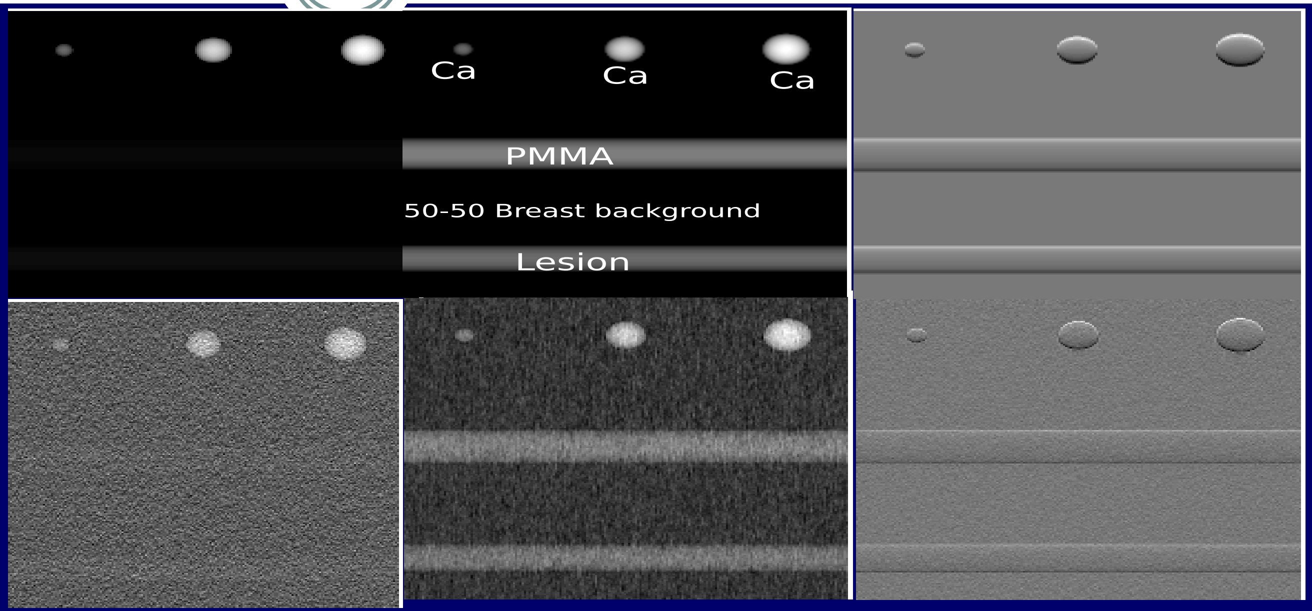

Absorption Phase Differential Phase

Mini Das and Zhihua Liang vol. 39, 21, Optics Letters, 2014

November 1, 2014 / Vol. 39, No. 21 / OPTICS LETTERS 6343

Spectral x-ray phase contrast imaging for single-shot retrieval of absorption, phase, and differential-phase imagery

Mini Das[1,*] and Zhihua Liang[2]

[1]Department of Physics, University of Houston, Houston, Texas 77004, USA

[2]Department of Biomedical Engineering, University of Houston, Houston, Texas 77004, USA

**Corresponding author: mdas@uh.edu*

Received August 27, 2014; revised September 25, 2014; accepted September 28, 2014;
posted September 30, 2014 (Doc. ID 221791); published October 31, 2014

In this Letter, we propose the first single-shot, noninterferometric x-ray imaging method for simultaneous retrieval

September 15, 2014 / Vol. 39, No. 18 / OPTICS LETTERS 5395

Approximated transport-of-intensity equation for coded-aperture x-ray phase-contrast imaging

Mini Das* and Zhihua Liang

Department of Physics, University of Houston, Houston, Texas 77204, USA

**Corresponding author: mdas@uh.edu*

Received June 16, 2014; revised July 30, 2014; accepted July 30, 2014;
posted August 4, 2014 (Doc. ID 214101); published September 12, 2014

Transport-of-intensity equations (TIEs) allow better understanding of image formation and assist in simplifying the

Propagation PCI – Additional Signatures

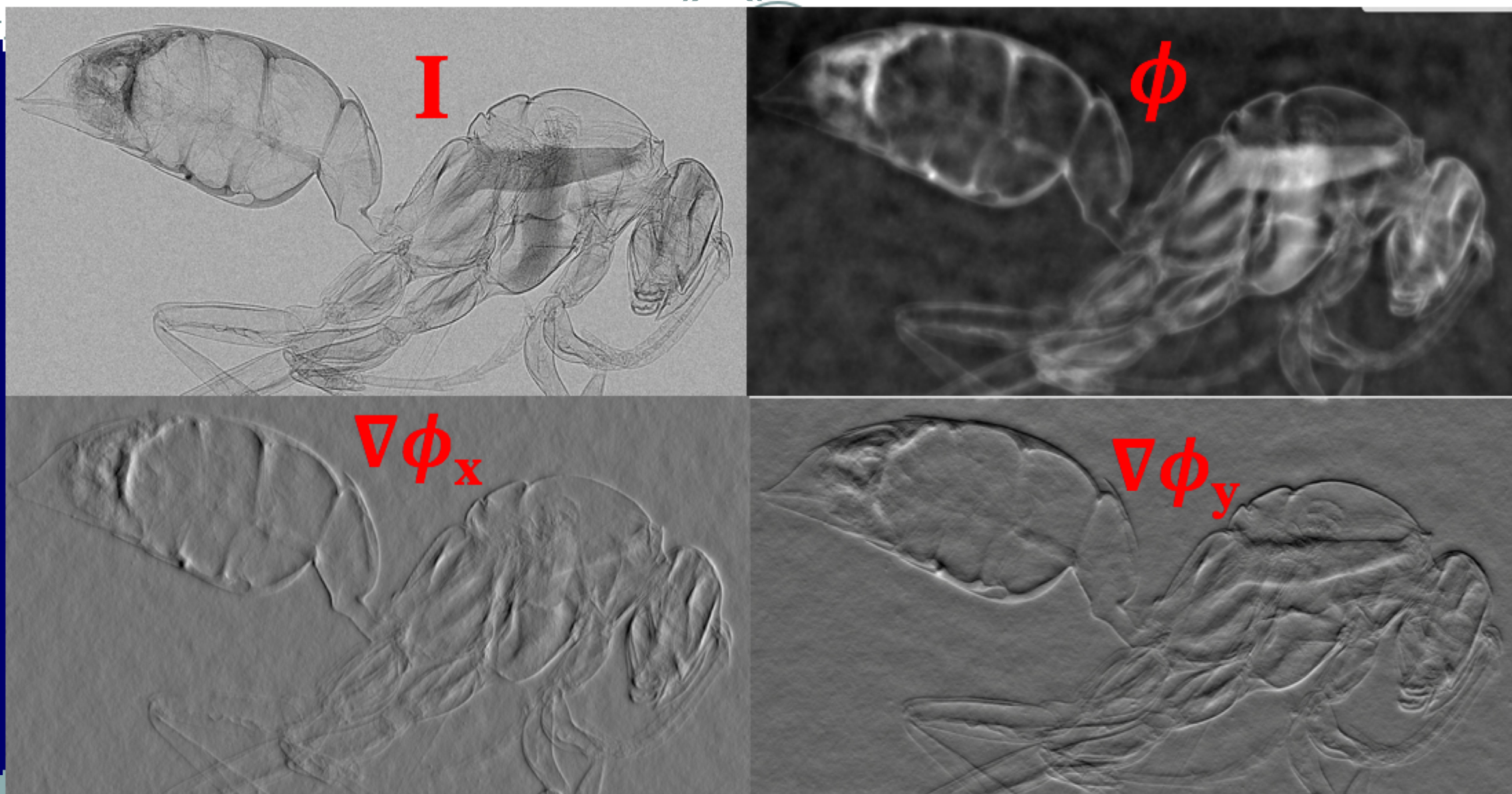

Quercus Emoryi/Emory Oak

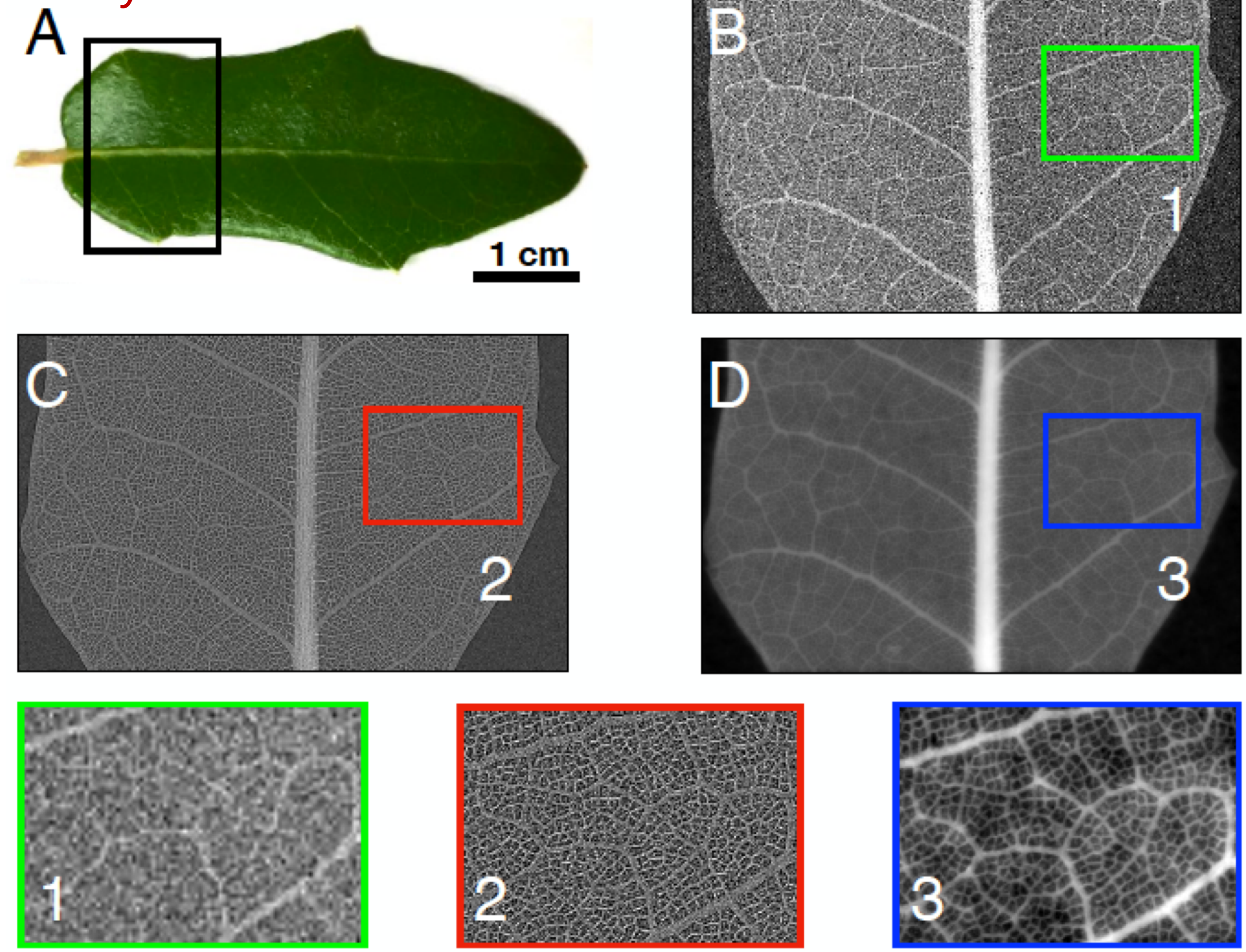

Low-Photon Count Phase Retrieval

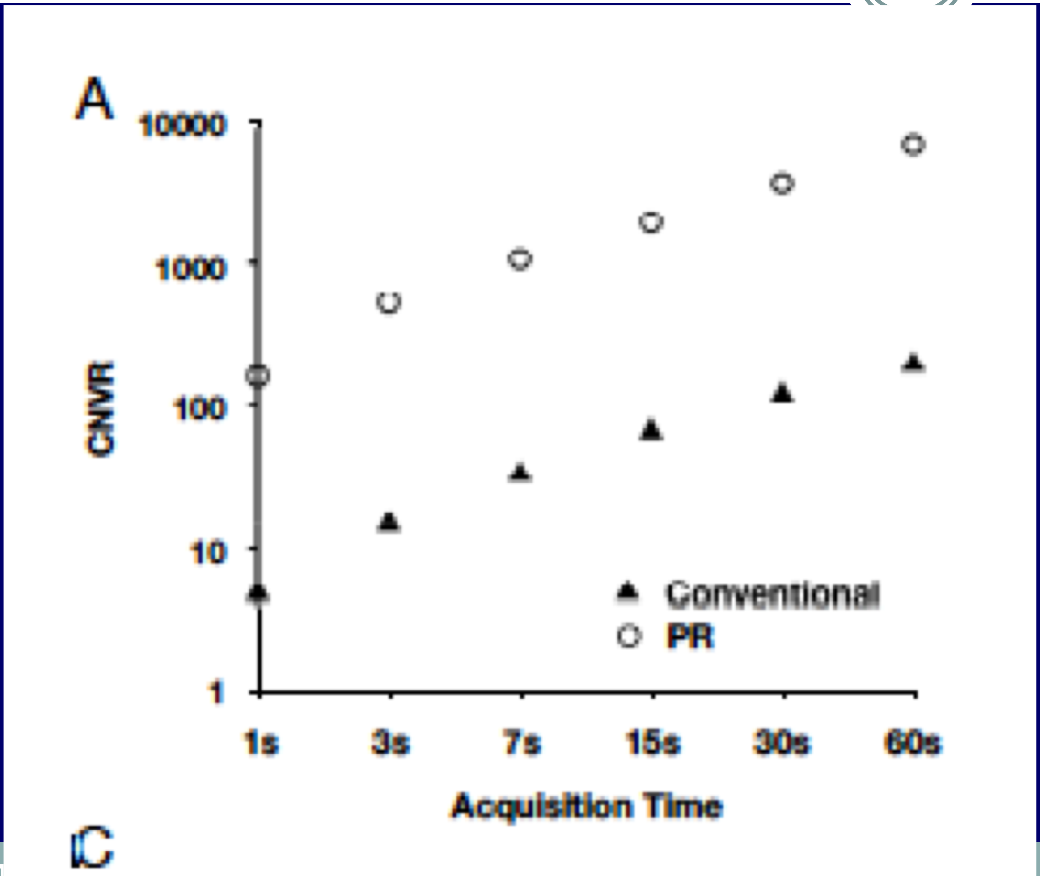

SPIE Medical Imaging 2020
Houston, TX

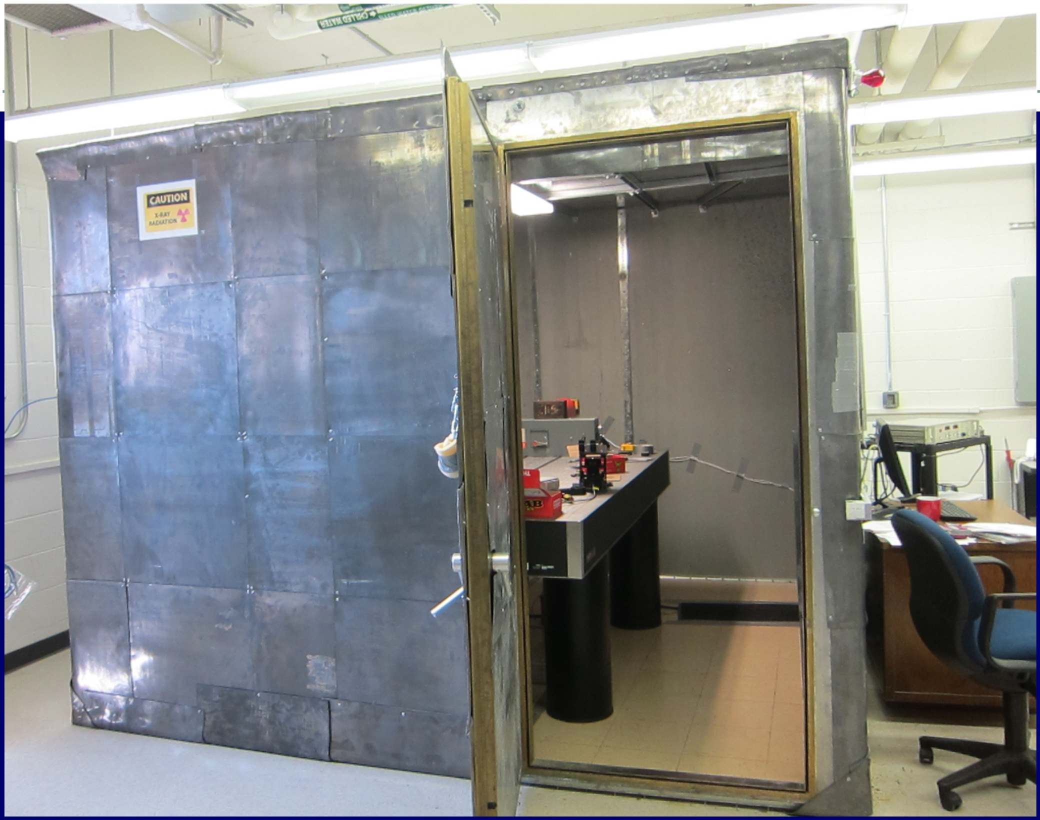
CAUTION

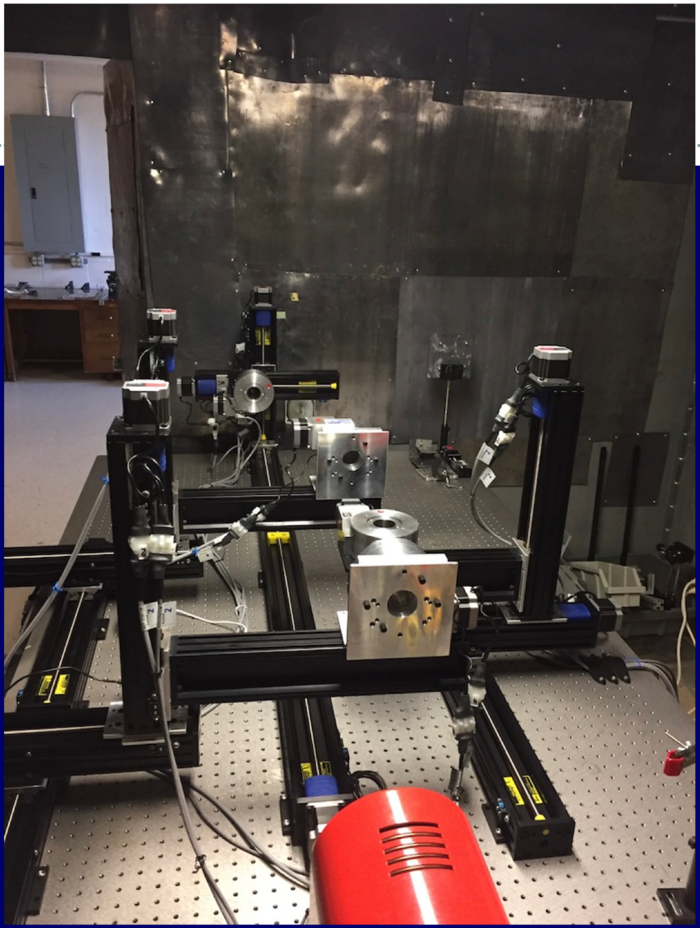

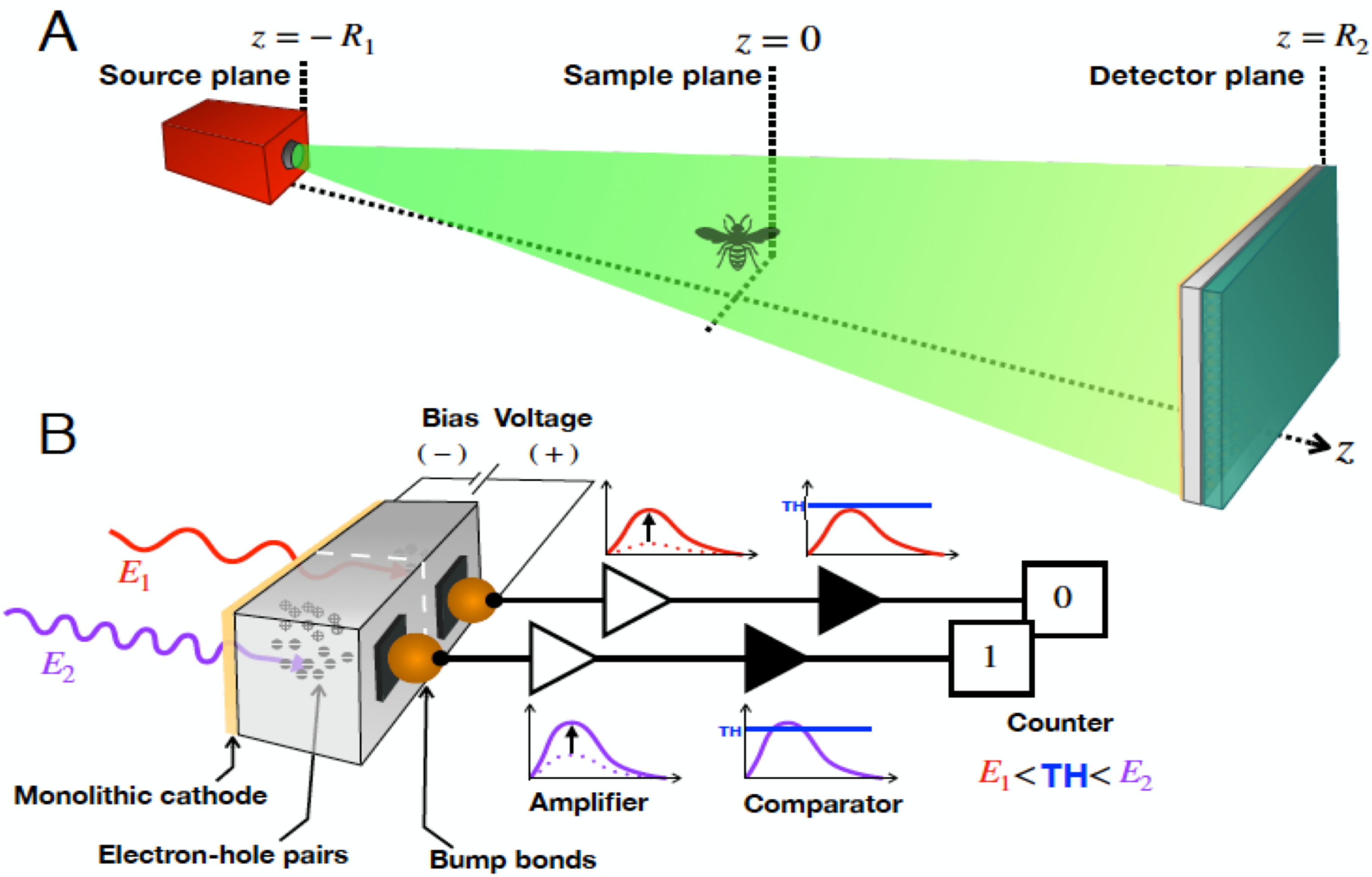

A
$z = -R_1$
Source plane
$z = 0$
Sample plane
$z = R_2$
Detector plane
z
B
Bias Voltage
(−)
(+)
E_1
E_2
TH
TH
0
1
Counter
E_1<TH<E_2
Monolithic cathode
Electron-hole pairs
Bump bonds
Amplifier
Comparator

M

Photon Counting Spectral Detectors

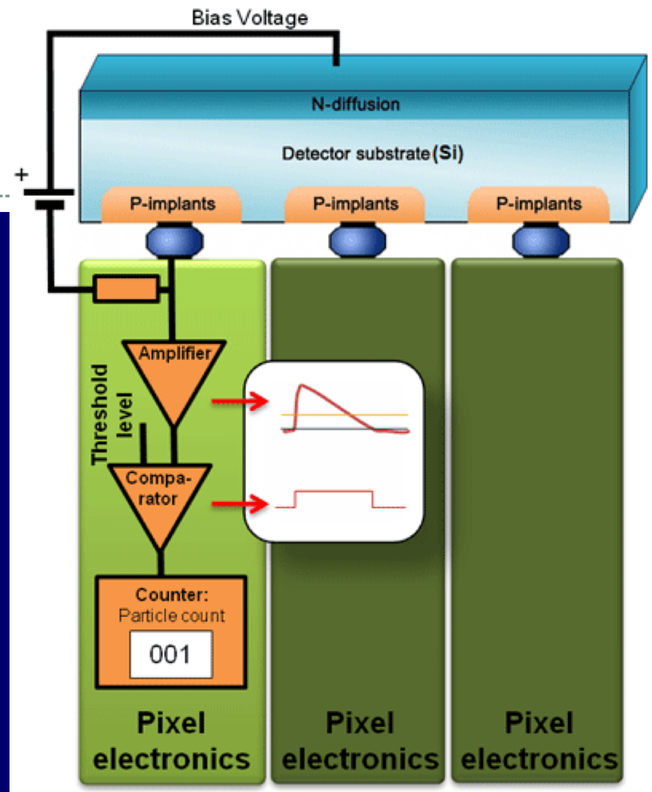

Images:
http://aladdin.utef.cvut.cz/

Spectral detection

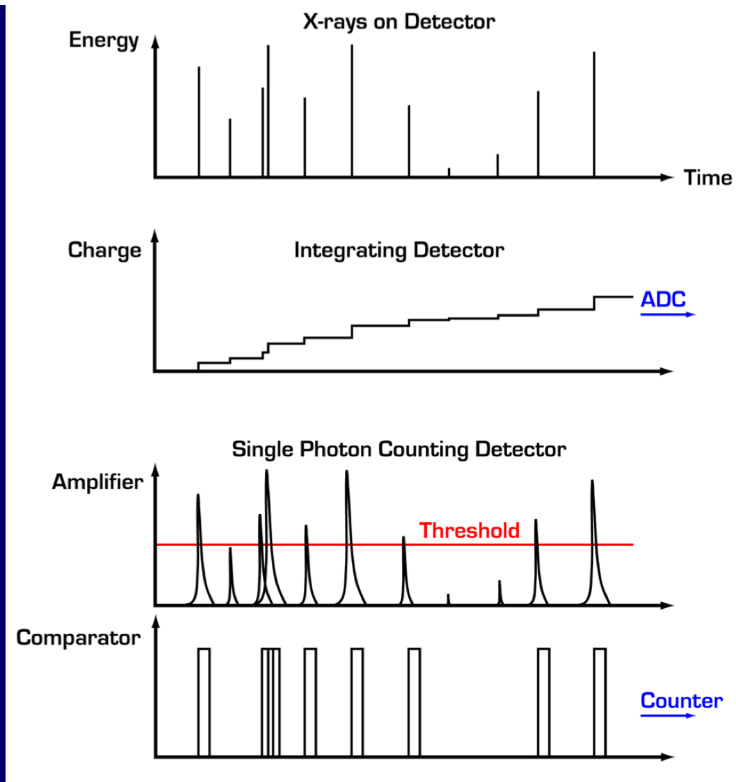

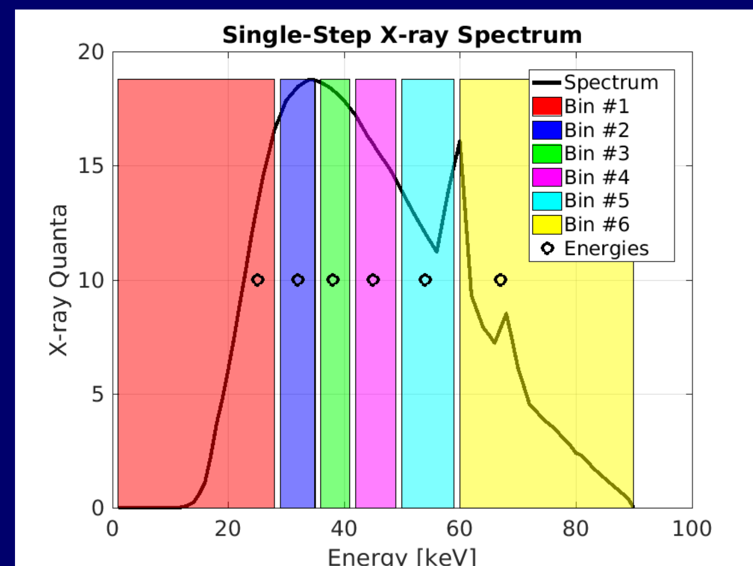

Vespucci, Das (2019) IEEE Transactions of Medical Imaging

Pulse Pile-up

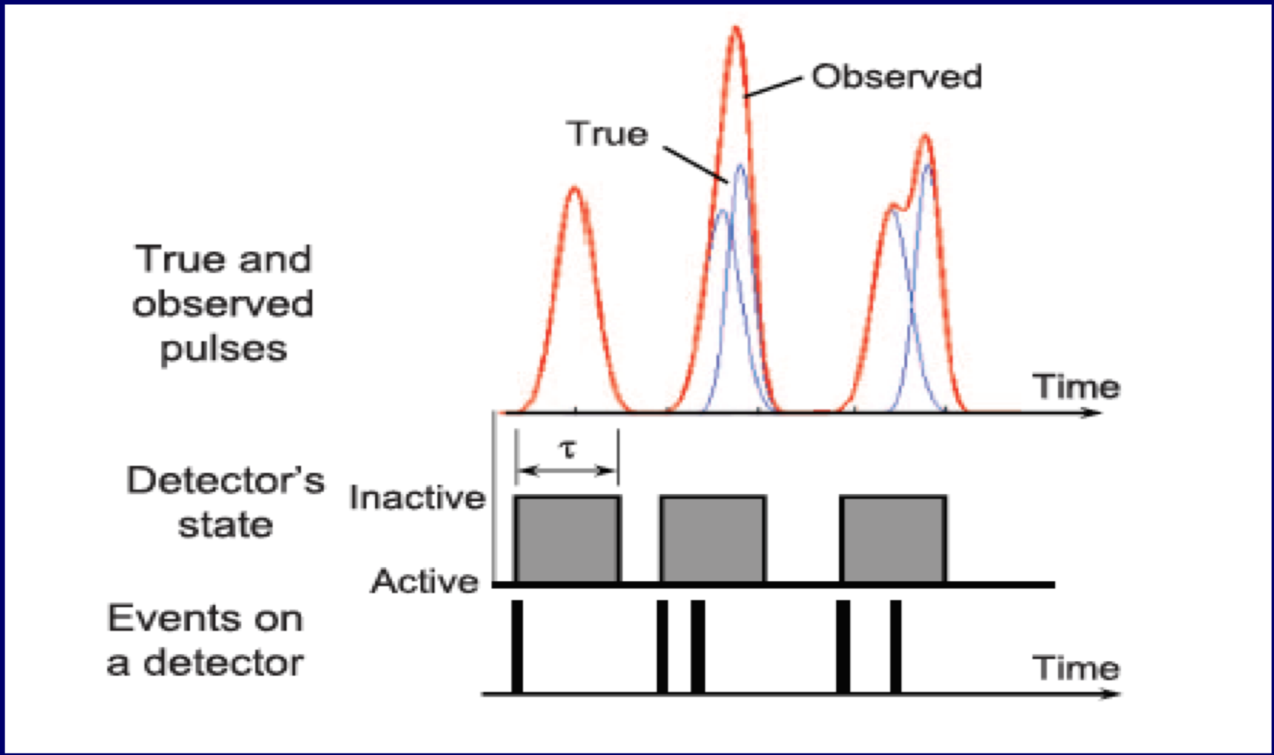

Charge Sharing

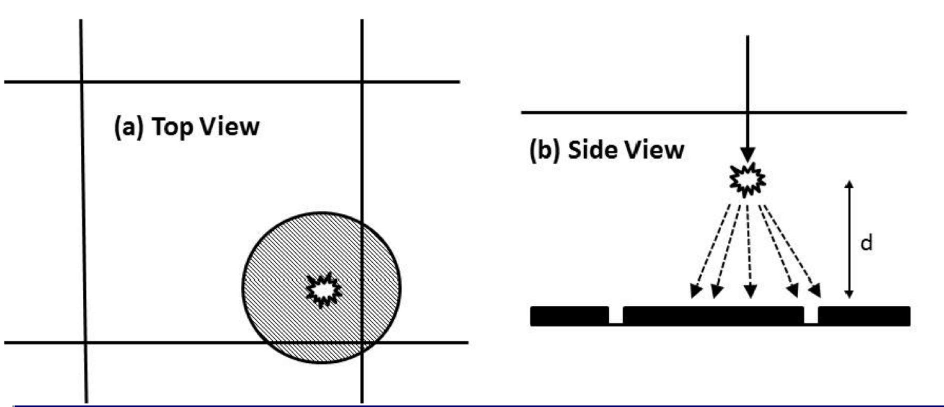

X-Ray fluorescence - Zr

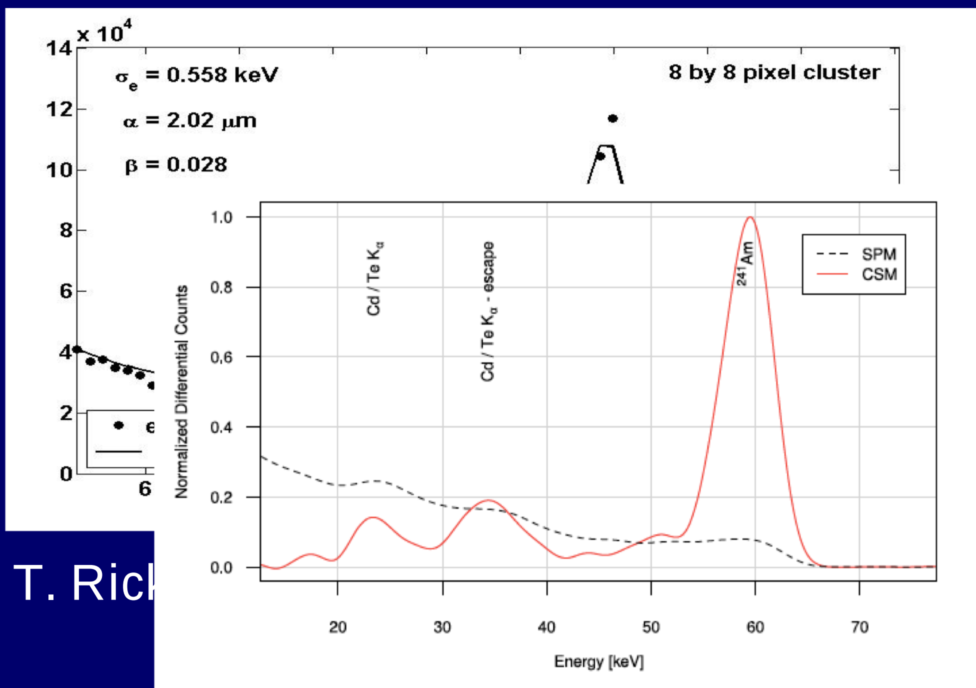

Charge Summing Mode

T. Rick

Sensor Material

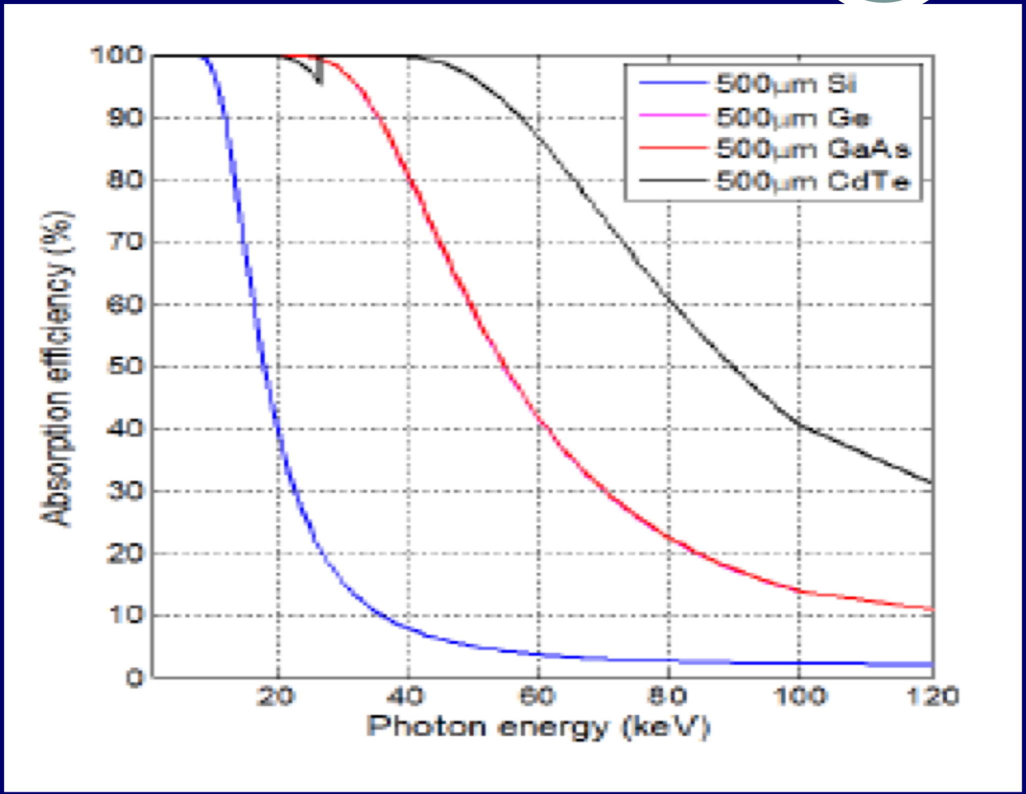

CdTe Sensor

Crystal defects
Temporal instability
Thermal instability

Single Quantum Processing

- Medipix Collaboration (CERN , Geneva)
- Medipix3RX – Current version
  - Flux tolerance ~ 70 million photons/second/mm^2
  - Includes charge sharing correction hardware
  - 2 – 8 energy bins at once
- Timepix – Time of arrival of detected photons

Time over Threshold (TOT Operation)

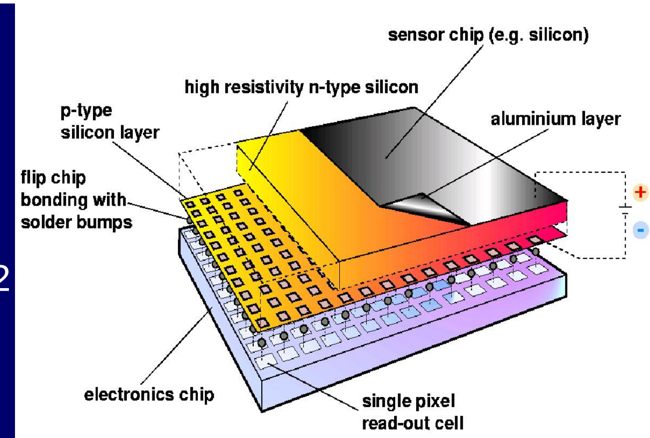

Physical Basis Functions

$$\mu(E,\vec{r}) = f_{ph}(E)\alpha_{ph}(\vec{r}) + f_C(E)\alpha_C(\vec{r}) + f_K(E)\alpha_K(\vec{r})$$

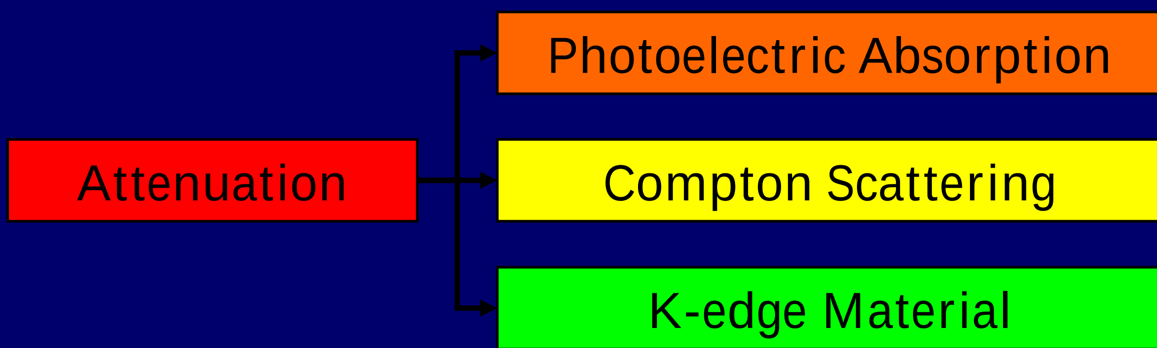

Image Domain Material Decomposition

$$\mu(E,\vec{r}) = \mu_1(E)\, f_1(\vec{r}) + \mu_2(E)\, f_2(\vec{r}) + \mu_3(E)\, f_3(\vec{r}) + \ldots$$

$\mu(E,\vec{r})$: *Linear attenuation coefficient* $[1/cm]$

$\mu_M(E,\vec{r})$: *Mass attenuation coefficient* $[g/cc]$

$f(\vec{r})$: *Volume fraction* $[0-1]$

Attenuation → Volume Fraction Material #1

Attenuation → Volume Fraction Material #2

Attenuation → Volume Fraction Material #3

$$\mu(E,\vec{r}) = \mu_{M1}(E)\, \rho_1\, f_1(\vec{r}) + \mu_{M2}(E)\, \rho_2\, f_2(\vec{r}) + \mu_{M3}(E)\, \rho_3\, f_3(\vec{r}) + \ldots$$

Single-Step Decomposition

$I(E_1,x,y)$ | $I(E_2,x,y)$ | $I(E_3,x,y)$ | $I(E_4,x,y)$ | $I(E_5,x,y)$ | $I(E_6,x,y)$

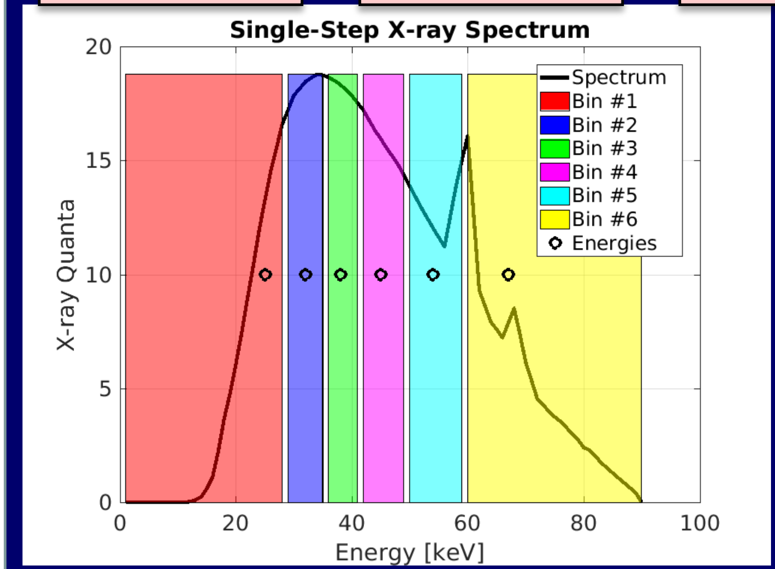

$$\mu(E,\vec{r}) = \mu_1(E)\, f_1(\vec{r}) + \mu_2(E)\, f_2(\vec{r}) + \mu_3(E)\, f_3(\vec{r}) + \ldots$$

Multi-Material Decomposition in Single Step

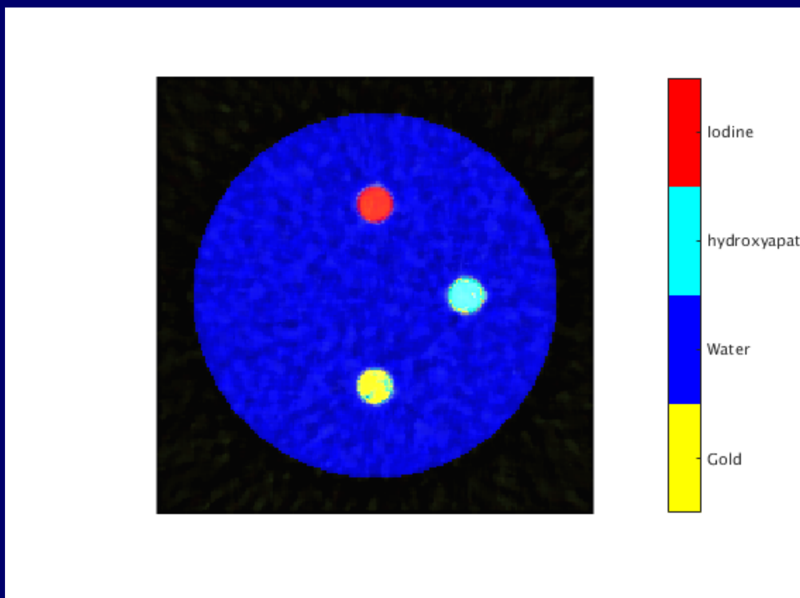

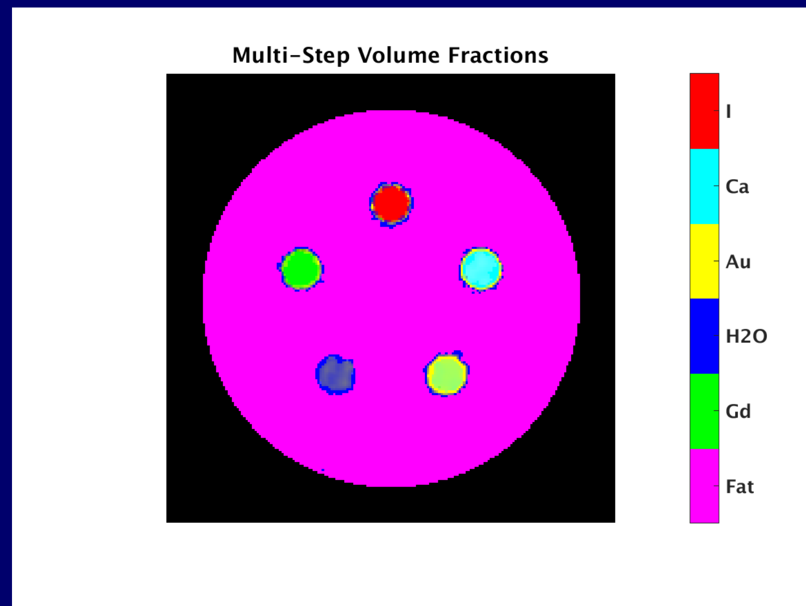

Nate Fredette et al. , SPIE (2017), PMB (2019)

Experimental Results

Multi-step Material Decomposition:
Fredette, Kavuri, Das (2017)(2019)

Applications:
Targeted drug delivery,
Multi-contrast imaging
Chemical imaging

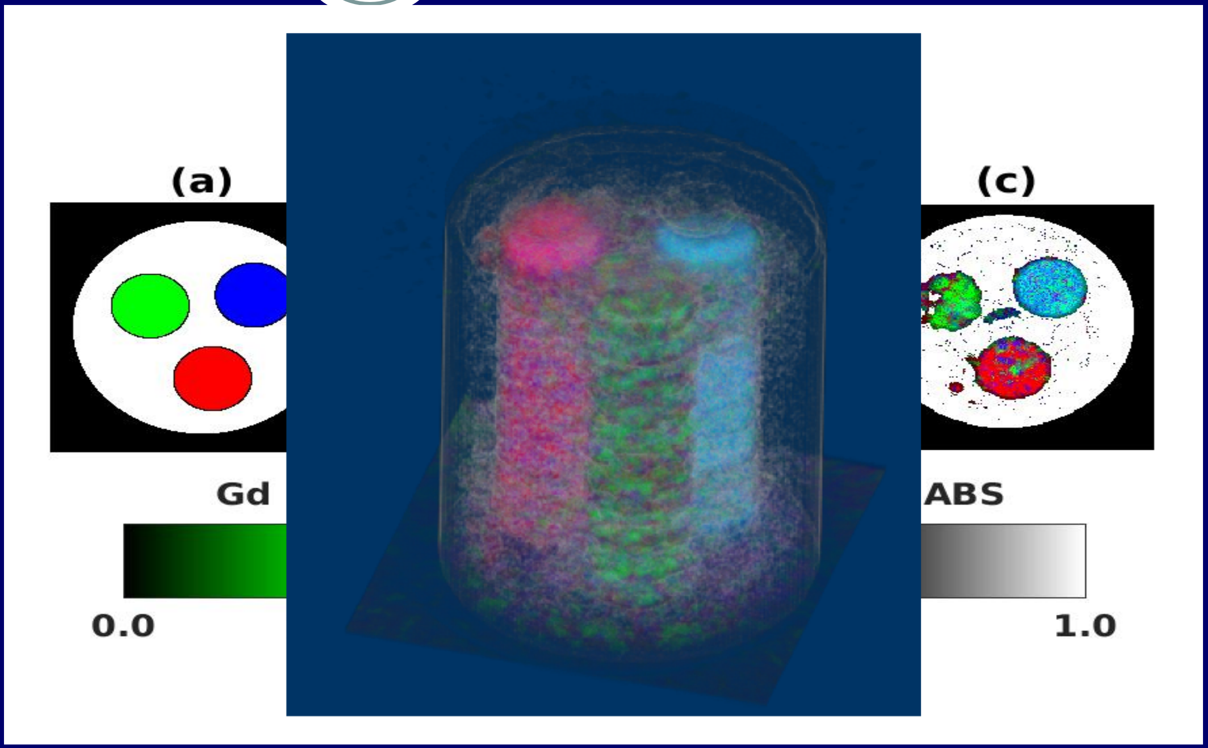

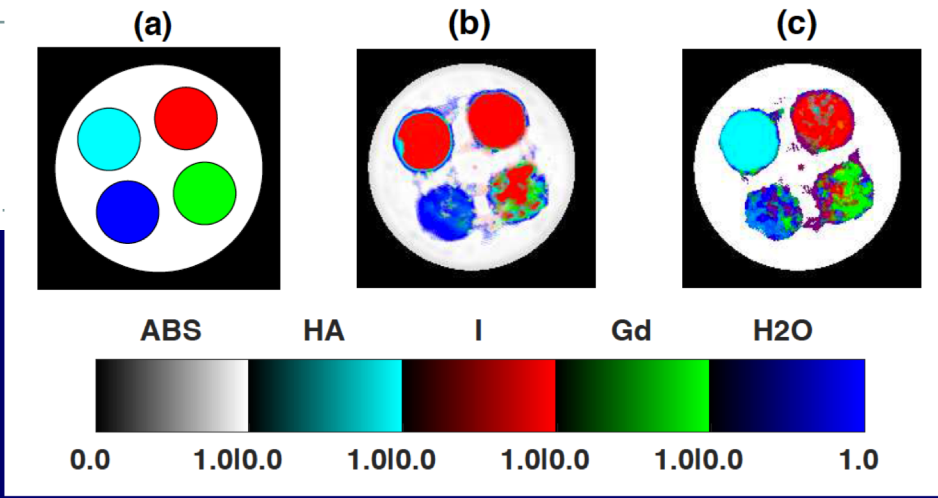

Silicon detector, 55 micrometer pitch

CdTe, 110 micrometer

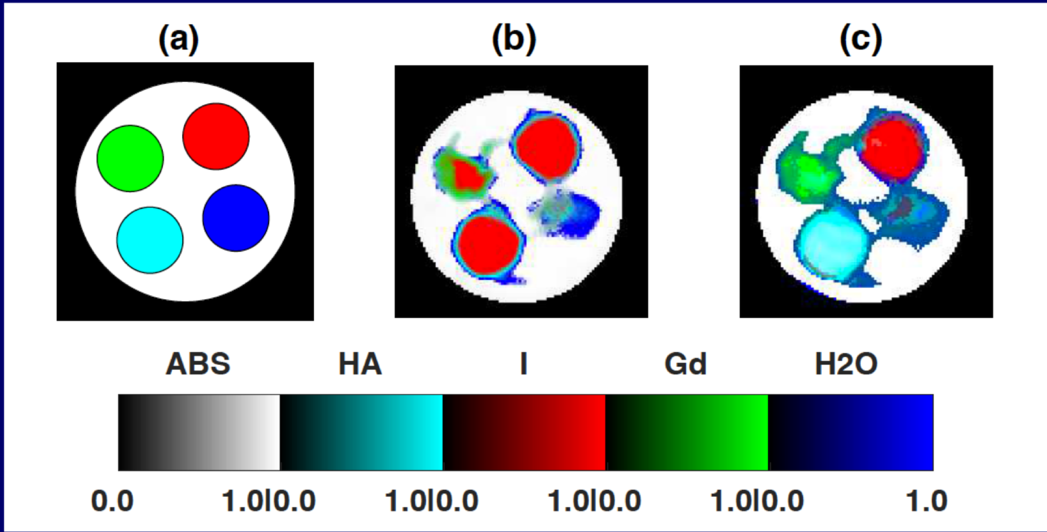

Highlighted in
Feature Article "X-Ray Images in Full Color
Nature Reviews Physics (2019)

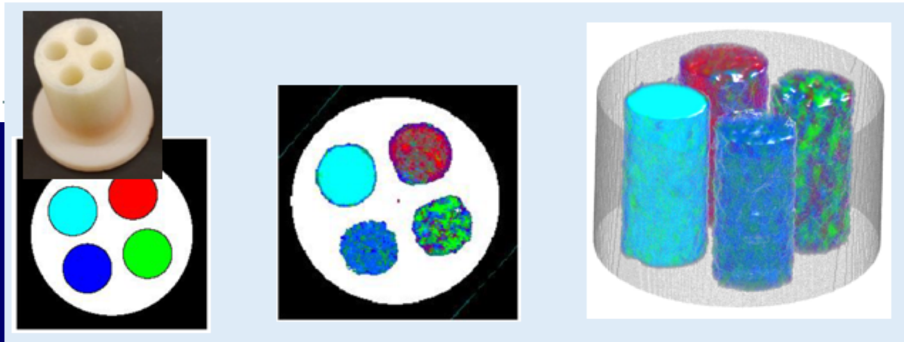

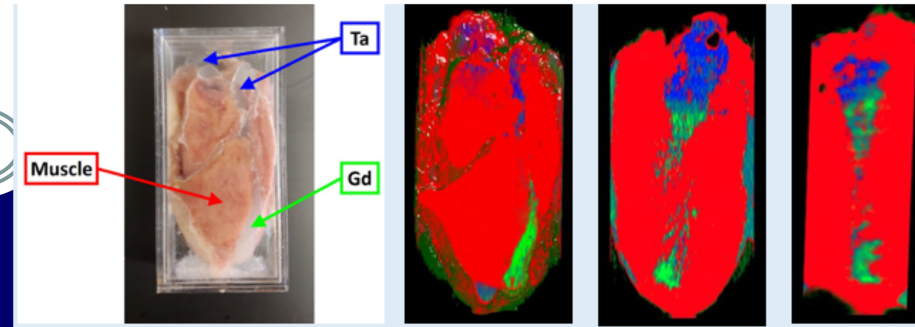

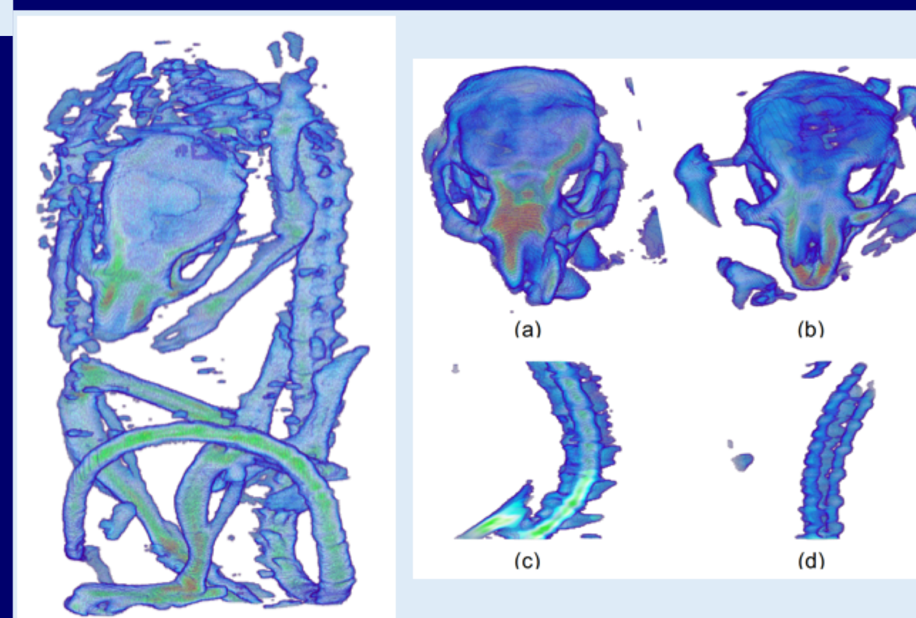

Iodine, Gd, water, Ca in plastic

Psychophysics

- Will lesion detectability improve with these emerging modalities?
- Task-based assessments
- Virtual clinical trials

-Machine learning

DBT- Image Acquisition and Reconstruction

- Three different densities of phantoms
  - 25%, 50%, 75%
- Projections acquired over four different arc spans
  - 30°, 45°, 60°, 75°
- For each arc span, we considered a number of projections ranging from 3 to 51

Phantoms created by P. Bakic, University of Pennsylvania

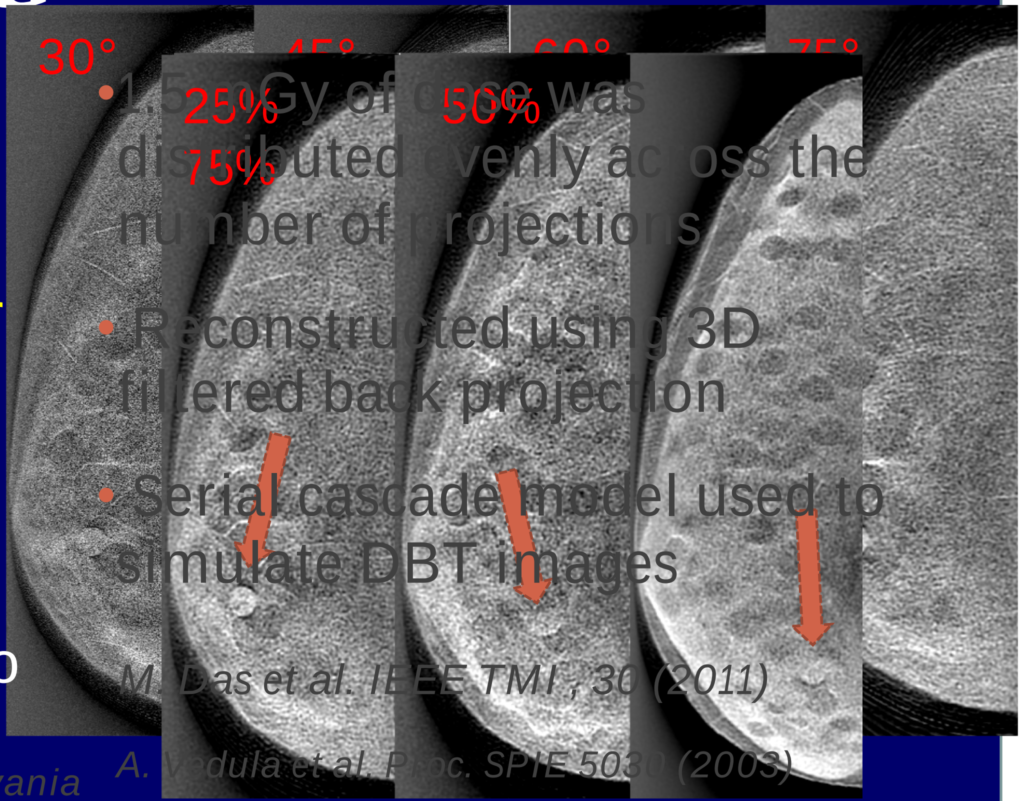

- 1.5 mGy of dose was distributed evenly across the number of projections
- Reconstructed using 3D filtered back projection
- Serial cascade model used to simulate DBT images

M. Das et al. IEEE TMI, 30 (2011)

A. Vedula et al. Proc. SPIE 5030 (2003)

Localization Receiver Operating Characteristic

LROC curve describes how well a human observer is able to detect a signal

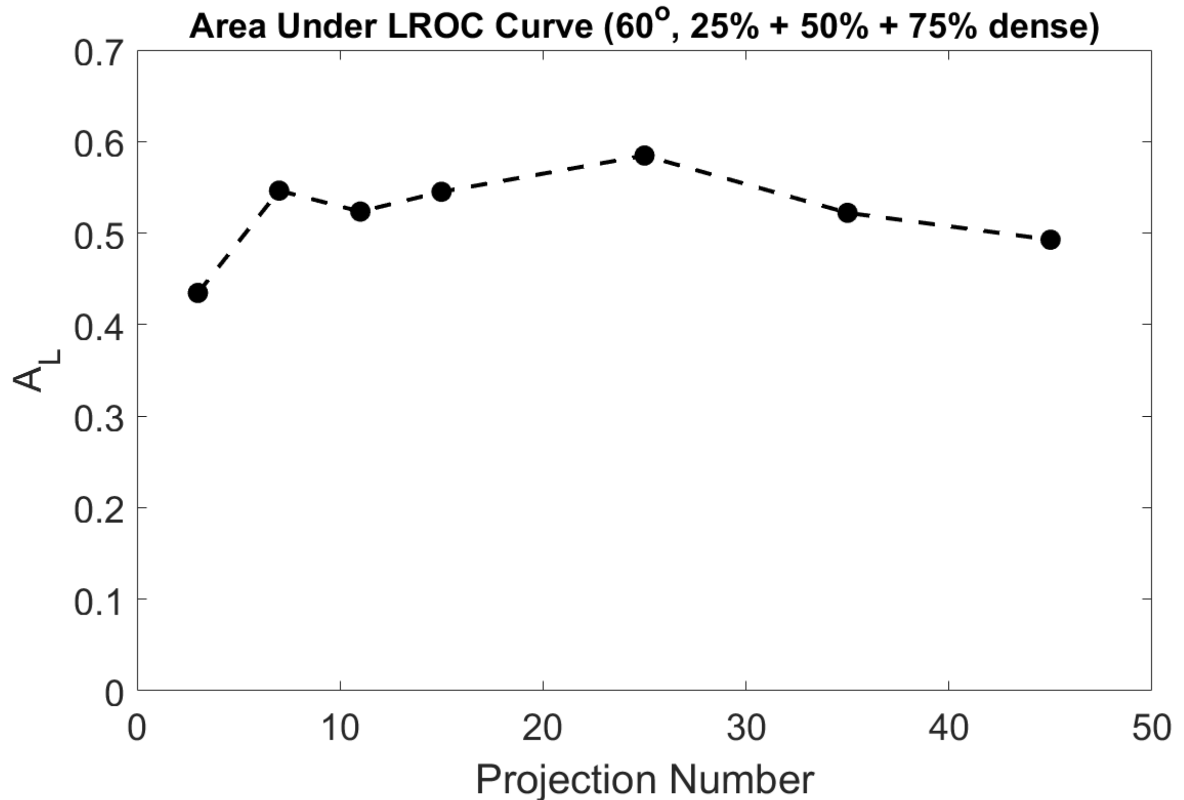

Das, Gifford (2016)

Image Texture

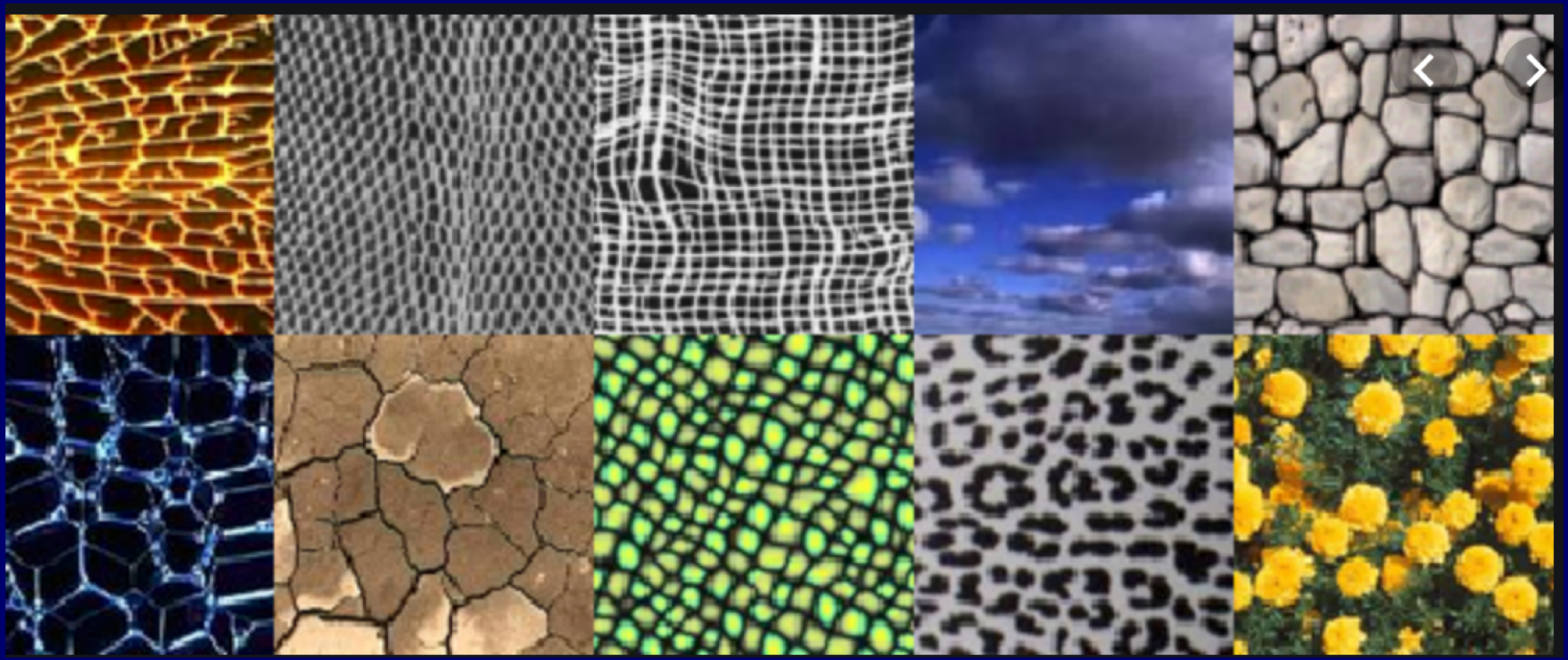

Texture Assessment

Texture and Perception?

Statistical featured computed in the Image

Nisbett, Das (2018)

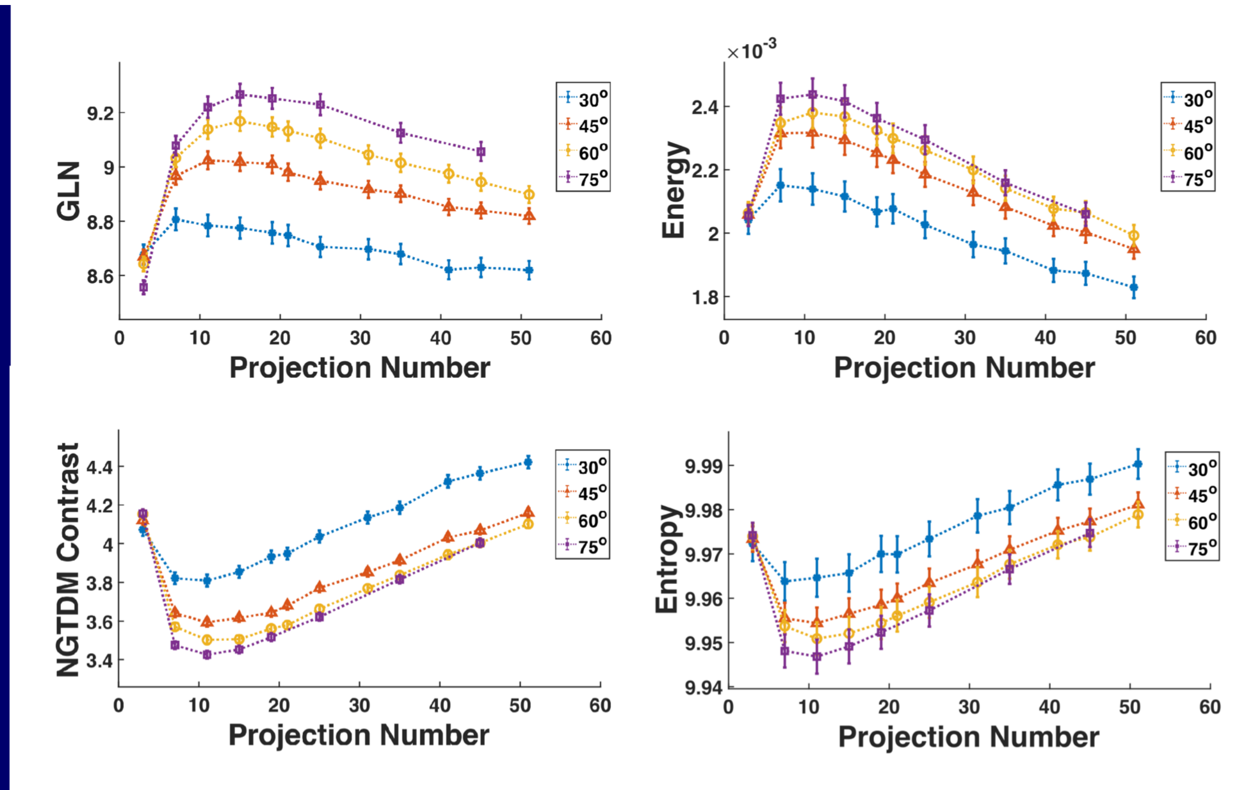

Observer Surrogates?

- Mathematical observer models (Gifford)
- Texture features. (Nisbett, Das (2017), (2018)
- Power spectral parameters (beta- anatomic noise)
- Physics of imaging - building blocks of machine learning tools

Summary

- Quantitative phase contrast imaging
- Spectral detectors
- Perception and image science will play an integral role in future device and algorithmic developments
- Towards x-ray microscopy with Timepix
- Color X-Ray

Research Opportunities

- Physics and engineering – experiments, models
- Computer Science – Image reconstruction, ML

- Breast Images, Pathology ...

- Biochemistry- Contrast Enhanced Imaging
- Mathematics- Inverse Problems

University of Houston

Contact:
Mini Das
mdas@uh.edu

Funding Support Acknowledgements

- National Science Foundation
- Department of Defense
- National Institute of Health